

ELECTROCHEMICAL DETECTION OF OXALIPLATIN INDUCED DNA
DAMAGE IN G-QUADRUPLEX STRUCTURES

A THESIS SUBMITTED TO
THE GRADUATE SCHOOL OF NATURAL AND APPLIED SCIENCES
OF
MIDDLE EAST TECHNICAL UNIVERSITY

BY

SILA CAN OSMANOĞULLARI

IN PARTIAL FULFILLMENT OF THE REQUIREMENTS
FOR
THE DEGREE OF MASTER OF SCIENCE
IN
CHEMISTRY

JULY 2022

Approval of the thesis:

ELECTROCHEMICAL DETECTION OF OXALIPLATIN INDUCED DNA DAMAGE IN G-QUADRUPLEX STRUCTURES

submitted by **SILA CAN OSMANOĞULLARI** in partial fulfillment of the requirements for the degree of **Master of Science in Chemistry, Middle East Technical University** by,

Prof. Dr. Halil Kalıpçılar
Dean, Graduate School of **Natural and Applied Sciences**

Prof. Dr. Özdemir Doğan
Head of the Department, **Chemistry**

Prof. Dr. Levent Toppare
Supervisor, **Chemistry, METU**

Assoc. Prof. Dr. Özgül Persil Çetinkol
Co-Supervisor, **Chemistry, METU**

Examining Committee Members:

Prof. Dr. Ali Çırpan
Chemistry, METU

Prof. Dr. Levent Toppare
Chemistry, METU

Assoc. Prof. Dr. Özgül Persil Çetinkol
Chemistry, METU

Prof. Dr. Sevil Savaşkan Yılmaz
Chemistry, Karadeniz Teknik Üni.

Assoc. Prof. Dr. Saniye Söylemez
Biomedical Engineering, Necmettin Erbakan Üni.

Date: 01.07.2022

I hereby declare that all information in this document has been obtained and presented in accordance with academic rules and ethical conduct. I also declare that, as required by these rules and conduct, I have fully cited and referenced all material and results that are not original to this work.

Name Last name : Sıla Can Osmanođulları

Signature :

ABSTRACT

ELECTROCHEMICAL DETECTION OF OXALIPLATIN INDUCED DNA DAMAGE IN G-QUADRUPLEX STRUCTURES

Osmanođulları, Sıla Can
Master of Science, Chemistry
Supervisor: Prof. Dr. Levent Toppare
Co-Supervisor: Assoc. Prof. Dr. Özgül Persil Çetinkol

July 2022, 64 pages

Oxaliplatin is an anticancer agent used in chemotherapy. As a platinum-based chemotherapeutic agent, it is known to induce DNA damage by generating intra- and inter-strand crosslinking mainly at N7 sites of adenine (A) or guanine (G) bases. Thus, a high dosage of Oxaliplatin results in different side effects. In order to understand the molecular mechanisms underlying these side effects and the drug resistance developing against Oxaliplatin, there is a need for rapid qualitative and quantitative determination of Oxaliplatin and the damage caused by it. Electrochemical based methods are one of the sensing platforms that can be preferred due to their sensitivity, simplicity and low cost. In this study, an electroanalytical platform for the detection of DNA damage caused by Oxaliplatin was constructed via using differential pulse voltammetry on gold nanoparticle (Au-NP)-modified graphite electrode. The surface characterization of the prepared electrodes was performed by scanning electron microscopy. The decrease in the intensity of the guanine oxidation signal with increasing Oxaliplatin concentration was taken as an indication of the binding of Oxaliplatin to DNA bases and used in the development of the detection platform with the dynamic range of 1.0 μM to 10.0 μM . The

Oxaliplatin induced damage could be detected as low as at 1.0 μM Oxaliplatin concentration under the optimized conditions. These results in here are expected to offer new insights into the investigations of DNA-Oxaliplatin interactions in the future studies.

Keywords: Oxaliplatin, DNA Damage, Electrochemical Detection, G-Quadruplex Structures, Differential Pulse Voltammetry

ÖZ

G-QUADRUPLEX DNA YAPILARINDA OXALİPLATİNİN YARATTIĞI DNA HASARININ ELEKTROKİMYASAL TESPİTİ

Osmanoğulları Sıla Can
Yüksek Lisans, Kimya
Tez Yöneticisi: Prof. Dr. Levent Toppare
Ortak Tez Yöneticisi: Doç. Dr. Özgül Persil Çetinkol

Temmuz 2022, 64 sayfa

Oksaliplatin kemoterapide kullanılan bir antikanser ajandır. Platin bazlı bir kemoterapötik ajan olan Oksaliplatin'in genelde adenin (A) veya guanin (G) bazlarının N7 bölgelerinde zincir içi ve arası çapraz bağlar oluşturarak DNA hasarını indüklediği bilinmektedir. Bu nedenle, yüksek dozda Oksaliplatin farklı yan etkilerin ortaya çıkmasına sebep olmaktadır. Bu yan etkilerin altında yatan moleküler mekanizmaları ve Oksaliplatin'e karşı gelişen ilaç direncini anlayabilmek için, Oksaliplatin'in ve neden olduğu hasarın hızlı bir şekilde kalitatif ve kantitatif olarak belirlenmesine ihtiyaç vardır. Elektrokimyasal yöntemler, duyarlılıkları, basitlikleri ve düşük maliyetleri nedeniyle tercih edilen tespit platformları arasında yer almaktadırlar. Bu çalışmada, altın nanoparçacık (Au-NP) ile modifiye edilmiş grafit elektrot üzerinde diferansiyel puls voltametri kullanılarak Oksaliplatin'in neden olduğu DNA hasarının tespiti için bir elektroanalitik platform geliştirilmiştir. Hazırlanan elektrotların yüzey karakterizasyonu, taramalı elektron mikroskobu ile gerçekleştirilmiştir. Oksaliplatin derişiminin artmasıyla guanin oksidasyon

sinyalinin şiddetinin azalması, Oksaliplatinin DNA bazlarına bağlanmasının bir göstergesi olarak alınmış ve dinamik aralığı 1.0 μM ila 10.0 μM olan algılama platformunun geliştirilmesinde kullanılmıştır. Bu koşullar altında, Oksaliplatin kaynaklı DNA hasarının 1.0 μM Oksaliplatinin varlığında rahatça tespit edilebildiği belirlenmiştir..

Sonuç olarak, elde edilen verilerin gelecekteki çalışmalar için DNA-Oksaliplatin araştırmalarına yeni bir bakış açısı sunması öngörülmektedir.

Anahtar Kelimeler: Oksaliplatin, DNA Hasarı, Elektrokimyasal Saptama, G-Dörtlü Yapılar, Diferansiyel Puls Voltametri

Dedicated to my family

ACKNOWLEDGMENTS

I would like to express my deepest gratitude to my supervisor Prof. Dr. Levent Toppare for his guidance, patience, and continuous support. I offer my sincere appreciation for the learning opportunities he provided in his research lab. It has been a great honor for me to be a part of Toppare family.

I am sincerely thankful to my co-supervisor Assoc. Prof. Dr. Özgül Persil Çetinkol for her guidance, support, and encouragement. She provided me invaluable advices and helped me in difficult periods of these project.

I would like to express my deep and sincere gratitude to Prof. Dr. Yasemin Arslan Udum for her continued encouragement in every issue. I am deeply grateful for her never-ending confidence in me.

I want to extend my thanks to Dr. Mehrdad Forough for his positive guidance, valuable suggestions, and comments.

I would also like to acknowledge Prof. Dr. Ali Çırpan, Prof. Dr. Sevil Savaşkan Yılmaz, and Assoc. Prof. Dr. Saniye Söylemez as the second reader of this thesis, and I am gratefully indebted to their very valuable comments on this thesis.

I am thankful to all the members of Toppare Research Group especially to Aybüke Deniz and Mustafa Yaşa for their help and friendship.

I am grateful to the academic staff of Department of Chemistry at METU for their support and guidance throughout my education.

This study was supported by Middle East Technical University Scientific Research Projects Coordination (METU BAP) with the project number of GAP-103-2021-10704. I would like to thank METU BAP for their support.

I would like to give my heartfelt thanks to my parents, who help me get by the most tough times and support me to pursue my dreams. Whenever I have difficulty in this period, they always motivate me. So glad that I have you.

TABLE OF CONTENTS

ABSTRACT	v
ÖZ.....	vii
ACKNOWLEDGMENTS	x
TABLE OF CONTENTS	xii
LIST OF TABLES	xiv
LIST OF FIGURES	xv
LIST OF ABBREVIATIONS	xvii
CHAPTERS	
1 INTRODUCTION	1
1.1 Electrochemistry	2
1.1.1 Electrodes	3
1.1.2 Voltammetry.....	4
1.2 Biosensors	6
1.2.1 Nanomaterials Used in Biosensor Design	8
1.2.2 Biological Components Used in Biosensor Design.....	9
1.3 DNA Damage	12
1.3.1 Factors Causing DNA Damage	12
1.3.2 Chemotherapeutic Agents and DNA Interactions	14
1.4 Electrochemical Detection Studies about DNA Damage in the Literature	17
2 EXPERIMENTAL STUDIES	21
2.1 Instrumentation	21

2.2	Materials and Methods	21
2.2.1	Pu22 G4 DNA Preparation	22
2.2.2	Oxaliplatin Preparation	22
2.2.3	Synthesis of AuNPs and Modification of the Working Electrode	22
2.2.4	Electrochemical Studies	23
2.2.5	Fluorometric Studies	27
2.2.6	Thermal Denaturation Studies	27
3	RESULT AND DISCUSSION	29
3.1	Electrochemical Studies	29
3.1.1	Optimization of the Amount of AuNPs Used in Modification of Graphite Electrode	30
3.1.2	Optimization of Pu22 G4 DNA Concentration on the Graphite Electrode	32
3.1.3	Optimization of Incubation Time for Pu22 G4 DNA and Oxaliplatin 34	
3.1.4	Optimization of Oxaliplatin Amount	36
3.1.5	Surface Morphologies	38
3.2	Fluorometric Studies	40
3.3	Thermal Denaturation Studies	41
3.4	Circular Dichroism Studies	43
4	CONCLUSIONS	45
	REFERENCES	47

LIST OF TABLES

TABLES

Table 2.1 Some Electrochemical Detection of DNA Damage Studies in the Literature.....	18
---	----

LIST OF FIGURES

FIGURES

Figure 1.1. An electrochemical cell and three-electrode sytem.....	3
Figure 1.2. Potential excitation signal types used in voltammetry.....	5
Figure 1.3. Typical differential pulse voltammogram.....	6
Figure 1.4. Purine bases of DNA.....	10
Figure 1.5. Pyrimidine bases of DNA.....	10
Figure 1.6. G-tetrad (on the left) and G-Quadruplex structures (right).....	12
Figure 1.7. Oxidation of guanine.....	13
Figure 1.8. Chemical structure of Oxaliplatin.....	16
Figure 2.1. Schematic representation of Au-NPs/Thiolated-DNA/GE construction	28
Figure 3.1. Differential pulse voltammograms (DPV) of 10.0 μ M Pu22 G4 DNA on the graphite electrode coated with varying concentrations of AuNPs. 1:0 w/o DNA sample represents the bare GE electrode with no DNA and 1:1, 1:2, 1:3, 1:4 represents the samples with decreasing AuNP concentration.....	31
Figure 3.2. Differential pulse voltammograms (DPV) of Pu22 G4 DNA at varying DNA concentrations (between 0.5 and 20.0 μ M). Three measurements were carried out in each cell using freshly cleaned and AuNPs modified electrodes.....	33
Figure 3.3. Differential pulse voltammograms (DPV) of Pu22 G4 DNA at varying concentrations.....	33

Figure 3.4. Differential pulse voltammograms (DPV) of 1.0 μM Pu22 G4 DNA incubated for varying time periods with 1.0 μM Oxaliplatin.....	35
Figure 3.5. Differential pulse voltammograms (DPV) of 1.0 μM Pu22 G4 DNA in the presence of varying concentrations of Oxaliplatin.....	36
Figure 3.6. Differential pulse voltammograms (DPV) of 1.0 μM Pu22 G4 DNA in the presence of varying concentrations of Oxaliplatin.....	37
Figure 3.7. Calibration curve of 1.0 μM Pu22 G4 DNA in the presence of varying concentrations of Oxaliplatin.....	37
Figure 3.8. SEM images of bare graphite electrode and AuNPs modified surfaces under optimized conditions with different scales.....	39
Figure 3.9. SEM images belonging to DNA on the electrode in the absence and presence of Oxaliplatin.....	40
Figure 3.10. Fluorescence Spectroscopy of varying molarity ratios of Pu22 G4 DNA:Oxp.....	41
Figure 3.11. Heating curve of varying molarity ratios of Pu22 G4 DNA:Oxp.....	42
Figure 3.12. Cooling curve of varying molarity ratios of Pu22 G4 DNA:Oxp.....	42
Figure 3.13. CD spectra of varying molarity ratios of Pu22 G4 DNA:Oxp.....	44

LIST OF ABBREVIATIONS

ABBREVIATIONS

AuNPs	Gold Nanoparticles
DNA	Deoxy Ribonucleic Acid
DPV	Differential Pulse Voltammetry
dsDNA	Double Stranded Deoxy Ribonucleic Acid
CD	Circular Dichroism
CPE	Carbon Paste Electrode
G4	G-Quadruplex
GCE	Glassy Carbon Electrode
GE	Graphite Electrode
OXP	Oxaliplatin
PGE	Pencil Graphite Electrode
RNA	Ribonucleic Acid
SEM	Scanning Electron Microscopy
SPE	Screen Printed Electrode
ssDNA	Single Stranded Deoxy Ribonucleic Acid
UV-Vis	Ultraviolet-Visible
VEGF	Vascular Endothelial Growth Factor

CHAPTER 1

INTRODUCTION

Nucleic acids are formed from nucleotides. They are molecules responsible for the expression of the genetic information. They are typically categorized into two groups based on their chemical structures: Ribonucleic Acid (RNA) and Deoxyribonucleic Acid (DNA). Both types of nucleic acids are formed by the polymerization of nucleotides. Phosphate and sugar units in macromolecular structure form the main backbone with the phosphodiester bonds [1]. DNA is one of the most important molecules where its structure has been elucidated in 1953 [2]. DNA is continuously exposed to damage due to several factors including exposure to ionizing radiation, exogenous and endogenous chemicals [3]. DNA damage is mostly repaired by DNA repair systems. However, certain levels of DNA damages cannot be repaired. In these cases, damages in the DNA molecule, in which genetic information is encoded and transmitted from generation to generation, cause mutations and, as a result, genomic instability and fatal diseases such as cancer occur [4]. Today, it is known that environmental factors can easily trigger genetic factors together with stress. Therefore, it is very important to design and use fast, reliable, sensitive, selective and economic analysis systems that can be used to detect DNA damage. In this context, biosensors often superior advantages over the time-consuming classical analysis systems [4].

A biosensor is defined as a device consisting of a biological sensing element and a transducer that outputs the signal [5]. Biosensors, as they are selective, sensitive and reliable analysis systems, are crucial in daily diagnosis applications. A biosensor converts the signal as the result of an interaction between the analyte and the sensing platform into a physical output, such as a change in electrical output. Biosensors

provide many superior advantages over other time-consuming classical analysis systems. Biosensor studies and applications have gained importance especially in recent years with the inclusion of developments in the field of nanotechnology [6]. Electrochemical biosensors are one of the most widely used types of biosensors.

Gold nanoparticles (AuNPs) are the most widely used nanoparticles in the construction of biosensors, especially for DNA detection. It has found that AuNPs increases the immobilization ability of DNA especially the thiolated DNA structures compared to a bare electrode [7].

In this thesis, a biosensor for the determination of DNA damage in G-quadruplex forming VEGF promoter DNA by chemotherapeutic agent Oxaliplatin was developed by using AuNPs modified graphite electrode. Changes in oxidation signals of guanine in the presence and absence of Oxaliplatin were determined using differential pulse voltammetry (DPV).

1.1 Electrochemistry

Electrochemistry examines the reactions which occur at the interface of an electrode surface as an electronic conductor, semiconductor or metal and an electrolyte solution [8]. In an electrochemical cell where an electrochemical process is maintained, the oxidation reaction occurs at the anode while the ion or molecular substance is reduced at cathode. Reactions happening at the electrode surface cause the transfer of electrons which lead to the generation of an electrical current. Electrochemical techniques provide important information about the mass transfer rate at the interface, the stoichiometry and rate of the charge transfer, the equilibrium and rate constants of a chemical reaction, the degree of chemisorption and adsorption, and redox properties of the species [9]. For example, Demirbas et al. used square wave voltammetry and cyclic voltammetry which are electrochemical methods, to investigate redox properties of newly synthesized phthalocyanine compounds [10]. Moreover, electrochemical methods are cheap in terms of

instrumentation and the amount of material used compared with other methods. Besides, these methods are sensitive, reliable, and fast response, and very easy to use. A typical electrochemical cell is given in Figure 1.1.

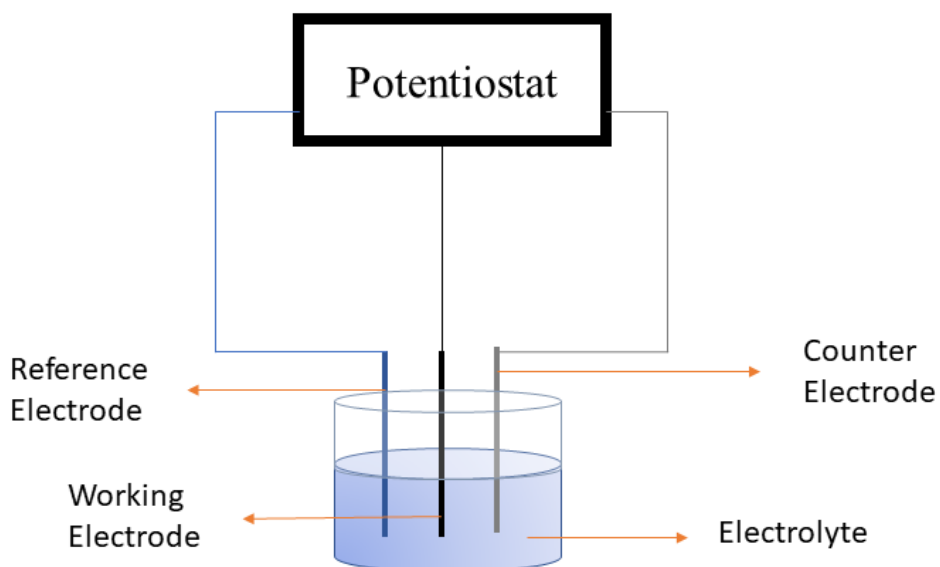


Figure 1.1. An electrochemical cell and three-electrode system

1.1.1 Electrodes

In electrochemical measurements, conventional three-electrode systems are widely used. Electrodes can be grouped as the reference electrode, the counter (auxiliary) electrode, and the working electrode [11].

1.1.1.1 Reference Electrode

The reference electrode is a type of electrode whose potential is known and kept constant during the whole chemical process and is insensitive to the composition of the analyte solution[12]. The reference electrode is a current carrier electrode which

ensures that the electricity from the source is transferred to the working electrode by passing through the electrolyte solution. The most common reference electrodes are standard hydrogen electrode (SHE), saturated calomel electrode (SCE), silver/silver chloride (Ag/AgCl) electrode [13].

1.1.1.2 Counter (Auxiliary) Electrode

The counter electrode is the electrode which provides constant potential precisely regardless of the analyte concentration. The potential provided by the counter electrode is continuously compared with voltage of the working electrode. The most common one is platinum electrode [14].

1.1.1.3 Working Electrode

The working electrode is the electrode where the oxidation-reduction reactions take place. This electrode is generally functionalized with the biorecognition element for the detection and/or surface modifiers for enhanced sensitivity. The surface of the working electrode can be modified with many materials which enable the signal enhancement by increasing the conductivity of the electrode or stabilizing its surface. The most common working electrodes are gold, mercury, platinum, glassy carbon, graphite, and carbon-based electrodes [15].

1.1.2 Voltammetry

Voltammetry is a method in which the current between working electrode and counter electrode is measured against the voltage that is varied within between the working and the reference electrode. The obtained current versus applied potential graph is called a voltammogram. In general, working electrodes used in voltammetry have very small surface area (a few millimeters or smaller) that results in increased polarization [16]. And as the result of the increased polarization, low detection limit

can be reached. The boundaries of potential that will be applied in order to examine the electrochemical behavior depends on the type of working electrode, solvent, and electrolyte used. The most common voltammetry types are linear sweep voltammetry, cyclic voltammetry, square wave voltammetry and differential pulse voltammetry (Figure 1.2) [16]

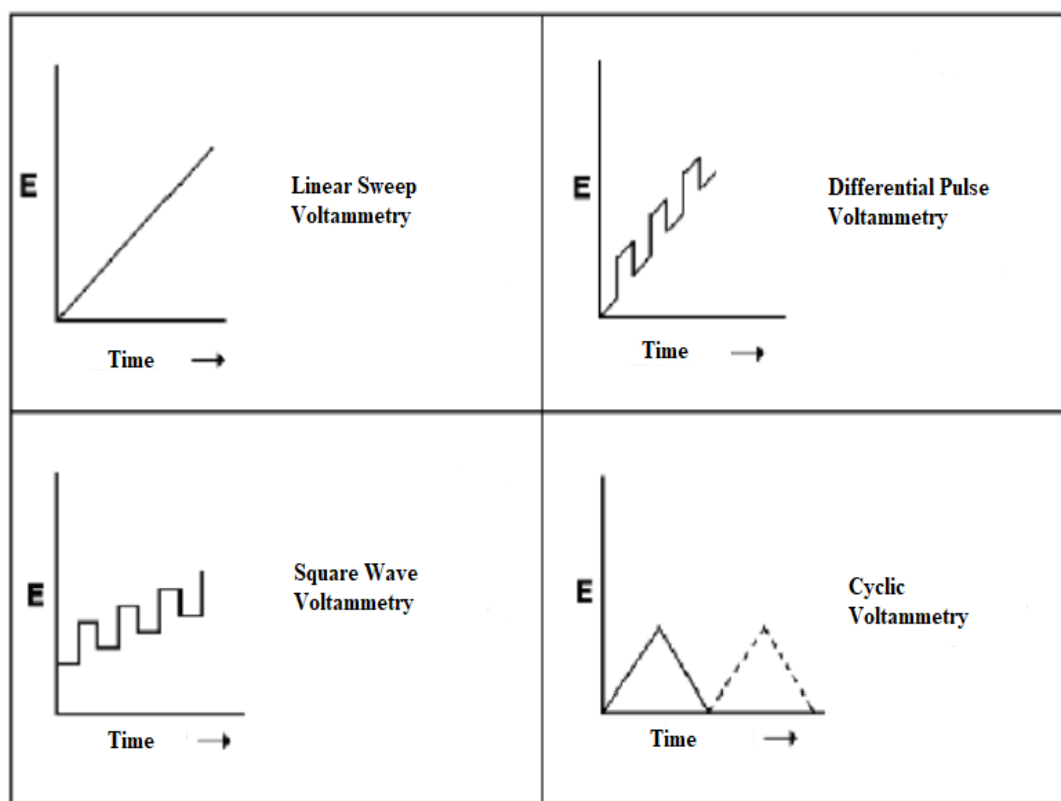


Figure 1.2. Potential excitation signal types used in voltammetry [16]

1.1.2.1 Differential Pulse Voltammetry

Differential pulse voltammetry (DPV) with low capacitive current and high Faradaic current is commonly preferred to reach low detection limit in voltametric studies. In differential pulse voltammetry, the ratio between these currents is increased,

resulting in low detection limits. Differential pulse voltammetry is especially useful in measuring the trace amounts of electroactive materials. The peak currents are directly proportional to the analyte concentration [17]. A typical differential pulse voltammogram is given in Figure 1.3.

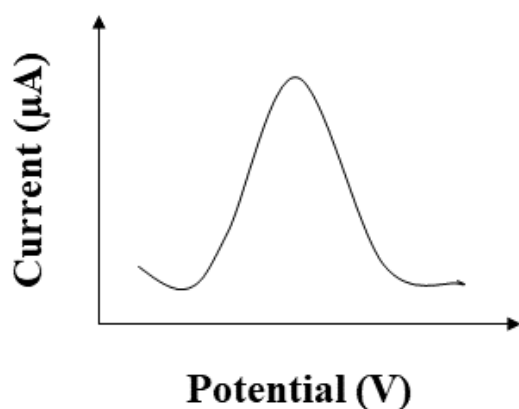


Figure 1.3. Typical differential pulse voltammogram

1.2 Biosensors

The “biosensor” term is defined as small sensing devices that are used to identify target substances to be analyzed in biological reactions by Thevenot [18]. After Clark and Lyons constructed an enzyme-based glucose biosensor in 1962, biosensor studies have accelerated [19].

A biosensor consists of two converters which are biochemical recognition system and a transducer. The biochemical recognition system interacts with the target analyte. A biochemical product may also be formed as a result of this recognition event. The second part of the biosensor, transducer, is responsible for converting this recognition event into a measurable numerical value [20]. A biorecognition element can be a nucleic acid [21], enzyme [22], antibody [23], bacteria [24] or a hormone [25]. A transducer which converts the recognition event to the readable value can

vary as piezoelectric (change of mass), thermal (heat change), optical (fluorometric) or electrochemical (potentiometric, voltametric, conductometric) depending on its type [26]. Optical biosensors are based on the measurement of absorbed or emitted light intensity resulting from the biorecognition event. Piezoelectric biosensors are used for the measurement of mass change which occurs after the interaction between the analyte and the biorecognition element. When the analyte is deposited on the piezoelectric crystal surface, resonance frequency of the crystal is changed which is accepted as the signal. Thermal biosensors are based on the measurement of heat change which occurs as the result of the interaction between the analyte and the biorecognition element. Electrochemical biosensors measure the electroactive signal which arises from the consumption or formation of the electrochemical species[27]. There are some drawbacks of all the different types of biosensors according to the area of utilization. For instance, optic biosensors cannot be used in the blurred areas. Thermal biosensors are not sensitive enough in systems where small heat changes occur [28].

There are some features that an ideal biosensor should have; [29]

- It should be selective.
- It should give a fast response.
- It should be easy to use and cheap.
- It should allow to work with small quantities.
- It should allow to get low detection limits.
- It should be stable and sensitive.
- It should be portable.

Biosensors have been utilized in many application areas such as medical, food, and environmental. For the patients who are suffering from diabetes, biosensors can be

used to detect glucose level in the blood [30]. Ethanol biosensors can be used to detect the amount of the alcohol in the alcoholic beverages as rum in food industry [31]. They can also be used in monitoring environmental agents which can carry serious health threat to humanity and ecosystem [32].

1.2.1 Nanomaterials Used in Biosensor Design

Nanotechnology is the ability to control a substance at the atomic, molecular, and supramolecular level. It can also be defined as the control of substances that have at least one dimension between 1 and 100 nanometers (nm). Application areas can vary from the development of new materials at the nanoscale to the direct control of matter at the atomic scale. Due to the unique properties of nanomaterials, nanotechnology research is rapidly developing in the fields of diagnosis, therapeutics, and drug delivery systems [33]. Thanks to nanotechnology, a wide range of materials with different properties can be prepared and their properties can be interfaced with biological molecules and other structures. Nanomaterials have superior physical and chemical properties and highly stable structures. Due to such advantages, interest in nanomaterials has increased in the last decades. With the inclusion of nanomaterials in detection platforms, very low amounts of substances can be detected, especially in biosensor studies, and at the same time, the analyte can be easily separated from species that interfere with very complex matrices. The development and applications of electrochemical DNA biosensor technologies based on nanomaterials have recently gained importance especially in the fields of genomics, medical diagnostics, and drug-DNA interactions [34]. And among the different types of nanoparticles, gold nanoparticles (AuNPs) have been widely used in DNA biosensors due to their high affinity in thiolated DNA [35].

AuNPs have a high surface to volume ratio and high surface energy, resulting in stable immobilization of many biomolecules that maintain their biological activity. In addition, AuNPs can provide fast and direct electron transfer between a wide variety of electroactive materials and electrode materials. In addition, their light

scattering properties and extremely high ability to amplify the local electromagnetic field make it possible to use AuNPs as signal amplification beacons in various biosensors [36]. Kang et al. used AuNPs as modification material to construct a DNA biosensor [37]. In their study, they used Thiolated DNA to take advantage of the affinity between gold and thiol groups. They performed hybridization of DNA in which the hybridization amount was increased greatly with the contribution of high surface to volume ratio of AuNPs. Bafrooei et al. used AuNPs for the modification of DNA biosensor to detect Bleomycin induced DNA damage in the presence of metal ions electrochemically [38]. In the study, they showed that the electrochemical signal was increased by AuNPs because of its high surface to volume ratio and good conductivity properties.

1.2.2 Biological Components Used in Biosensor Design

Biosensors can be designed for the detection of biological components such as antibodies, enzymes, tissues, nucleic acids and cells. The very same components can also be used in the design of the biosensors as capturing elements for the target analyte [39].

1.2.2.1 Nucleic Acids

Nucleic acids are macromolecules in which the genetic information is carried and preserved from generation to generation. Deoxyribonucleic acid (DNA) and ribonucleic acid (RNA) are the most common types. Building blocks of nucleic acids are called nucleotides. Nucleotides consist of a pentose sugar (deoxyribose in DNA and ribose in RNA), phosphate group and a nitrogenous base. Nitrogenous bases are pyrimidine or purine bases (Figure 1.4 and Figure 1.5). Nucleotides are named according to the nitrogenous base that they contain. The pyrimidine bases are uracil (U), cytosine (C), and thymine (T); purine bases are guanine (G), and adenine (A). While deoxyribonucleic acid (DNA) contains adenine, guanine, cytosine and

thymine bases, ribonucleic acid (RNA) contains adenine, uracil, guanine and cytosine bases [40].

In genomic DNA, two nucleotide strands are wound around each other forming the double helical structure. In that structure, the bases in opposite strands are hydrogen bonded to each other; adenine bonded with thymine, and cytosine bonded with guanine. Phosphodiester bonds form the skeletal structure of DNA and RNA [1]. Other than the double helical structure reported by Watson and Crick in 1953, DNA and RNA can adopt different structures as quadruplex structures. Understanding all the structural properties of nucleic acids is very important in terms of new and effective DNA-targeting drug design, detecting some hereditary diseases and understanding mutations in genes [41].

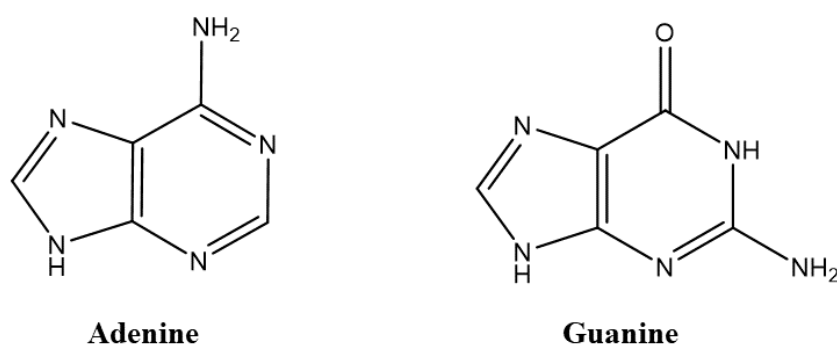


Figure 1.4. Purine bases of DNA

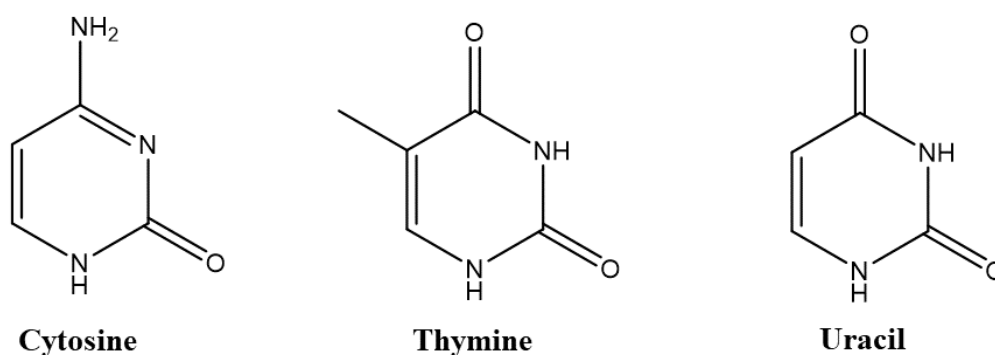


Figure 1.5. Pyrimidine bases of DNA

1.2.2.1.1 The G-quadruplex Structures

Among the various types of DNA structures, G-quadruplex structure (Figure 1.6) was first discovered in the 1960s and has been an important area of research and application ever since [42]. It is known that guanine rich sequences can form what is known as G-quadruplex structures [43]. Tetrads are generated from the association of four guanine bases through Hoogsteen hydrogen bonding and then the G-quadruplex structures are formed from the stacking of these tetrads. The guanine tetrads have central cavities which are occupied by various cations such as sodium or potassium. Cations in the central cavity are stabilizing the G-quadruplex structure [44].

G-quadruplex structures are known to exist in the promoter regions of numerous genes, including oncogenic promoters [45]–[47]. Vascular Endothelial Growth Factor (VEGF) promoter is one of these promoter regions known to be forming G-quadruplex structures and is associated with cancer [48]–[50]. For tumor growth and metastasis, angiogenesis which is the formation of new blood vessels, is important as it provides oxygen and nutrients to proliferating tumor cells, thereby promoting tumor progression [51]. This is regulated by many angiogenic factors, such as fibroblast growth factors, vascular endothelial growth factors (VEGF), and angiopoietins [52]. Among them, VEGF has been recognized as a key mediator of tumor angiogenesis by stimulating proliferation, migration, survival, and permeability of endothelial cells [53]. Sun et al., in their study, show that the G-rich strand in VEGF region can form G-Quadruplex structures by using the electrophoretic mobility shift assay, dimethyl sulfate foot printing technique, the DNA polymerase stop assay, circular dichroism spectroscopy, and computer-aided molecular modeling [54]. G-Quadruplex structures are located upstream of the promoter region in human VEGF gene and have multiple binding sites for transcription factors. This tract can form specific G-quadruplex structures and potentially allows transcriptional control of the VEGF promoter through G-quadruplex ligands [55]. Since human VEGF expression is primarily regulated at the

transcriptional level, it is of great importance to design drugs that target VEGF and the G-quadruplex forming promoter region.

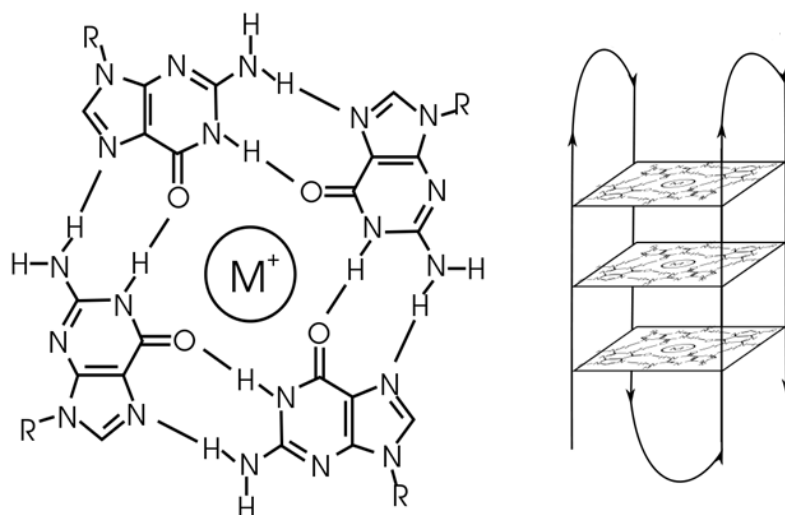


Figure 1.6. G-tetrad (on the left) and G-Quadruplex (right) Structures

1.3 DNA Damage

DNA is continuously exposed to damage due to several factors including exposure to ionizing radiation, exogenous and endogenous chemicals[56]. DNA damage is mostly repaired by DNA repair systems. However, certain levels of DNA damages cannot be repaired. In these cases, the cells will mostly program themselves towards apoptosis, the programmed cell death. Yet, certain types of DNA damages can escape the repair system and can cause permanent change in genetic material which are called the mutations [57].

1.3.1 Factors Causing DNA Damage

Spontaneous or inherited gene mutations, inflammation, detoxification process, free radical formation during energy production of mitochondria as factors resulting from

natural cellular metabolism; UV light, electromagnetic waves, ionizing radiation, air pollution, chemotherapeutic agents as environmental factors may cause DNA damage. Reactive oxygen, carbonyl and nitrogen species are known to form radicals that cause DNA damage. Especially reactive oxygen species cause important DNA lesions such as mutagenesis and carcinogenesis which is called oxidative DNA damage [58]. In general, reactive oxygen species produced in cells contain free radicals such as hydrogen peroxide, hydroxyl radical and superoxide anion. In particular, the hydroxyl radical is highly unstable and reacts rapidly and randomly with most biological molecules. As a result, such oxidants can damage cells by initiating chemical cell reactions [59].

DNA damage causes the formation of the radical cation guanine. Among nucleic acid bases, guanine is the most easily oxidized due to its lowest ionization potential [60]. The 8-oxo-dG is one of the most abundant DNA lesions, and it is considered as a biomarker of oxidative stress [61]. Therefore, guanine is most likely oxidized by electron transfer. Electron transfer induces the formation of a guanine radical cation followed by 8-oxo-dG formation via hydration and oxidation [62]. In addition to 8-oxo-dG, other products such as 2-aminoimidazolone and 2,2-diaminooxazolone can be obtained through the formation of guanine radical cations [63].

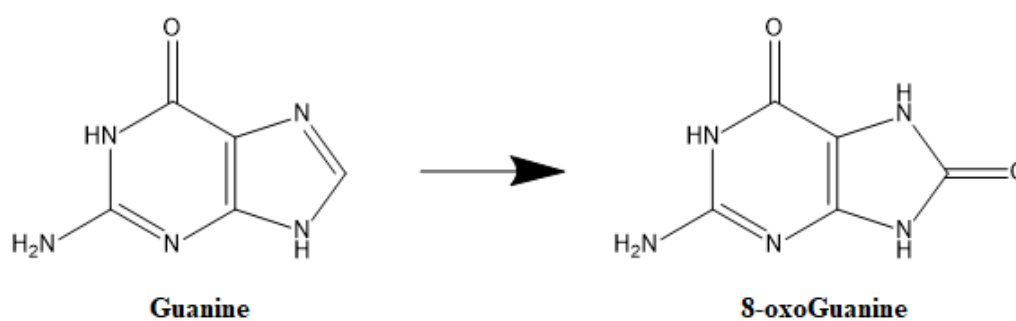


Figure 1.7. Oxidation of guanine

Alkylation of the bases and the crosslinking are also two other common types of DNA damage observed in the nature. Alkylating agents are the oldest class of anticancer drugs still widely used and they play an important role in the treatment of various types of cancer [64]. Alkylating agents are widely distributed in the environment and are also produced endogenously as byproducts of cellular metabolism. They damage DNA or RNA bases, which can be cytotoxic, mutagenic or neutral to the cell. Cytotoxic lesions block replication, interrupt transcription or initiation of apoptosis, while mutagenic lesions miscode and cause mutations in newly synthesized DNA [65]. DNA crosslinking are among the most toxic DNA damages [66]. DNA crosslinking damage occurs when crosslinkers covalently link two nucleotide residues from the same DNA strand (intra-strand crossing) or opposite strands (inter-strand crossing). Crosslinks can cause mutations and DNA rearrangements that can lead to cell death [67]. Chemotherapy today also relies on DNA damage. Many of the agents used in chemotherapy cause this type of DNA damage, as described below.

1.3.2 Chemotherapeutic Agents and DNA Interactions

Cancer is the uncontrolled and abnormal growth and proliferation of cells. Each cell has a certain number of cell divisions throughout its life. Cancer cells form tumors by aggregation which can compress, infiltrate, or destroy normal tissues [68]. Cancer cells can spread to other parts of the body through blood or lymph circulation. This spread of cancer to other parts of the body is called metastasis [69]. Different types of cancers grow at different rates, show different ways of spreading, and respond to different treatments. For this reason, different treatments are applied to the cancer patients considering the type of cancer. Chemotherapy means treatment with drugs which are called anticancer agents. Many chemotherapeutic agents induce direct or indirect DNA damage while targeting rapidly dividing cancer cells. Anticancer drugs generally bind to DNA in two ways: non-covalently and covalently. Non-covalent binding is generally classified as groove binding and intercalation. Covalent binding

is an irreversible event which may cause cell death by inhibiting DNA processes such as transcription and replication [70]. Mitomycin C, Daunomycin, Cisplatin, Oxaliplatin are some of the chemotherapeutic agents. While Mitomycin C and Daunomycin are binding to DNA non-covalently, Cisplatin and Oxaliplatin are binding covalently.

Platinum based anticancer agents have been extensively used to treat tumors for several decades [71]. The era of platinum-based chemotherapy began in the 1960s when Barnett Rosenberg accidentally discovered the effects of Cisplatin on cancer cells [72]. Platinum-based drugs have a great importance in the treatment of cancer and are currently used in almost half of all chemotherapeutic treatments, often in combination with other anticancer agents [73]. They exert their effects on cancer cells by attacking the genomic DNA and causing damage by alkylation and cross-linking beyond repair so that the programmed cell death will be initiated. Platinum based anticancer agents bind mainly to guanine nucleotides covalently specifically to N7 of guanines and induce the formation of inter- or intra- strand crossing [74]. Since these crossings cannot be repaired, the cell initiates apoptosis. Cisplatin is the first platinum-based anticancer agent discovered by Bernotti in 1965 [75]. One of the most important problems of Cisplatin is its severe dose limiting side effects resulting from its indiscriminate uptake by all rapidly dividing cells including tumor cells as well as bone marrow cells. Also, it causes pressure on the kidneys to remove the drug from the body [73]. Some other side effects are nephrotoxicity, neurotoxicity, myelosuppression, and ototoxicity [76]. Furthermore, numerous types of cancer cells may develop resistance to Cisplatin [77], [78]. Finally, Cisplatin has been found to suffer from poor tumor penetration, with evidence suggesting that clinically effective doses of the drug are delivered only to tumor cells located closest to the blood vessels [79]. Because of these disadvantages, new analogues of Cisplatin were developed. Among them, second generation Carboplatin and third generation Oxaliplatin (Figure 1.8) are the most successful ones and are currently used not only in clinical trials, but also as standard therapy for certain tumor types. Especially Oxaliplatin has demonstrated antitumor activity in Cisplatin-resistant cell lines and tumor types that

are self-resistant to both Cisplatin and Carboplatin [80]. Like Cisplatin, Oxaliplatin is known to form crosslinks on adjacent guanine bases or between guanine and adenine. Oxaliplatin-DNA adducts are more effective in inhibiting DNA synthesis than Cisplatin [81]. Because of these factors, Oxaliplatin has different spectrum of activity compared to Cisplatin or Carboplatin. Currently, Oxaliplatin is used for the treatment of the colorectal cancer, and it is being evaluated in clinical trials for the treatment of gastric, pancreatic, breast and non-small cell lung cancers [73].

To understand the drug resistance that develops against platinum-based drugs and the molecular mechanisms underlying the side effects of these drugs, there is a for rapid qualitative and quantitative determination of the damage caused by these drugs [82]. The need for fast, sensitive, easy, and low-cost analytical detection platforms to determine the occurrence of DNA damage and the parameters on the formation of DNA damage has made this field one of the interesting topics in recent years.

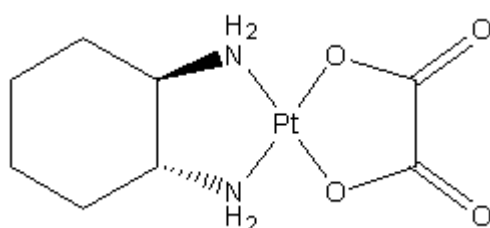


Figure 1.8. Chemical structure of Oxaliplatin

On the other hand, although studies on Cisplatin and Cisplatin-induced DNA damage have mostly focused on genomic DNA, it has been revealed in recent years that this group of drugs also disrupts G4 structures and damages them [83], [84]. It has been suggested that telomeric DNAs containing TTAGGG sequences may be a more obvious target than normal DNA due to their richness in guanine. For example, in the plasmid containing 800 base TTAGGG sequences, it was observed that there was more platinum insertion in this region than in other regions. Likewise, those with

long telomeres in melanoma cells were more resistant to Cisplatin. For this reason, it has been suggested that Cisplatin-telomer interactions may play an important role in understanding drug resistance [85]. On the other hand, there are also studies in the literature showing that Cisplatin does not prefer guanine-rich sequences [86]. There are a couple of Cisplatin studies presented in the literature regarding the interactions of Cisplatin with G-quadruplex telomeric DNA structures [87], [88]. Studies of Cisplatin and its derivatives with other guanine-rich G-quadruplex structures are almost non-existent. One of the few studies reported was the investigation of the interactions between Cisplatin and the C-MYC G4 helix conducted by He [89]. To the best of our knowledge, there are no studies reported so far on the interactions of Oxaliplatin with G-quadruplex forming VEGF structures.

1.4 Electrochemical Detection Studies about DNA Damage in the Literature

Electrochemical methods are one of the preferred platforms for probing the DNA Damage due to their low cost and high sensitivity [90]. Several electrochemical platforms were developed for probing chemotherapeutic agents and the DNA damage caused by them (Table 1.1). For instance, Topkaya et al., using a pencil graphite electrode, performed an electrochemical biosensor study for the damage caused by irinotecan on DNA. In this study, using the differential pulse method, the decrease in guanine oxidation peak and the damage caused by irinotecan on DNA were shown [91]. Yardım et al. developed an electrochemical biosensor using graphene oxide modified glassy carbon electrode to demonstrate the damage Cisplatin causes on dsDNA. In this study, which was carried out using the differential pulse method, the decrease in the guanine oxidation peak and the damage caused by Cisplatin on dsDNA were shown with 0.3 μM limit of detection [92].

Table 1.1 Some Electrochemical Detection of DNA Damage Studies in the Literature

Drug	DNA	Technique	Electrode	References
Cisplatin	dsDNA	CV	ITO	[93]
Cisplatin				[94]
& Carboplatin	dsDNA	SWV	SPE	
Anthracycline	dsDNA	CV & DPV	GCE	[95]
Mitomycin C	dsDNA	CV	CPE	[96]
Cisplatin	ssDNA			[97]
& Carboplatin	dsDNA	CV	GE	
Carboplatin	ssDNA	DPV	GCE	[98]
Fulvestrant	dsDNA	DPV	PGE	[99]
Cyclophosphamide	ssDNA	DPV	PGE	[100]
Leuprolide	dsDNA	Adsorptive Stripping Voltammetry	PGE	[101]

To the best of our knowledge, electrochemical studies on the damage caused by Oxaliplatin on G-Quadruplex DNA structures have not been carried out and a detection platform has not been established so far. In this thesis, for the first time, a biosensor for the detection of Oxaliplatin damage on G-Quadruplex DNA was developed by using AuNPs modified graphite electrode. G-quadruplex forming VEGF promoter region (Pu22) was exposed to Oxaliplatin, and the damage occurred

was investigated by changes in oxidation signals of guanine in the presence and absence of Oxaliplatin using DPV.

CHAPTER 2

EXPERIMENTAL STUDIES

2.1 Instrumentation

Electrochemical experiments were performed by using differential pulse voltammetry utilizing PSTrace 5.7 software system of Palm Sens potentiostat (EmStat 3, Netherlands). The three-electrode system consisted of the graphite electrode (3.0 mm diameter) as the working electrode, Ag wire as the pseudo reference electrode and platinum wire as the auxiliary electrode.

Fluorescence measurements were performed by Cary Eclipse Fluorescence spectrophotometer (Santa Clara, CA, USA).

Thermal denaturation experiments were performed by Cary 8454 photodiode array spectrophotometer with Agilent 89090A peltier (Santa Clara, CA, USA).

For surface morphology of the all biosensor layers, scanning electron microscope (SEM) (JEOL JSM-6400 model) at METU Central Laboratory was used.

2.2 Materials and Methods

Gold (III) Chloride Trihydrate ($\text{HAuCl}_4 \cdot 3\text{H}_2\text{O}$, 99.9%), Trisodium Citrate Dihydrate ($\text{Na}_3\text{C}_6\text{H}_5\text{O}_7 \cdot 2\text{H}_2\text{O}$, 99%), Cysteamine ($\text{NH}_2\text{CH}_2\text{CH}_2\text{SH}$), Acetic Acid (CH_3COOH), Sodium Acetate (NaCH_3COO) and Sodium Chloride (NaCl) were obtained from Sigma-Aldrich (St. Louis, MO, USA); Oxaliplatin (OXp, $\text{C}_8\text{H}_{14}\text{N}_2\text{O}_4\text{Pt}$, 98.7%) is obtained from Sicor De Mexico, S.A. DeC.V. (Lerma, Mexico) companies. All other reagent grade chemicals for the preparation of buffer solution and supporting electrolytes were obtained from Merck and Sigma.

2.2.1 Pu22 G4 DNA Preparation

Thiolated 5ThioMC6-D (5'-CGG GGC GGG CCG GGG GCG GGG T-3') oligonucleotide was purchased from Biomers.net GmbH (Ulm/Donau, Germany) the biopolymer factory. Non-thiolated Pu22 DNA oligonucleotides used in the experiments were purchased from Integrated DNA Technologies (IDT) (Coralville, IA, USA). UV-Vis absorption spectroscopy was utilized to calculate the concentrations of the oligonucleotides by using the Pu22 molar extinction coefficients; $\epsilon_{260} = 205000$. Stock solution of DNA (36.8 μM) was prepared in 25mM K-phosphate buffer with 70mM KCl. To allow formation of G4 DNA structures, these solutions were annealed by heating in a water bath at 92-93 °C for 5 minutes and allowed to cool overnight. More diluted solutions of Pu22 G4 DNA including the samples used in CD and Fluorescence measurements were prepared with 50mM acetate buffer solution (pH 4.8) containing 0.02M NaCl.

2.2.2 Oxaliplatin Preparation

Oxaliplatin ($\text{C}_8\text{H}_{14}\text{N}_2\text{O}_4\text{Pt}$, 98.7%) was obtained from Sicor De Mexico, S.A. De C.V. (Lerma, Mexico). Oxaliplatin concentration was calculated by UV-vis absorption spectroscopy using Oxp; $\epsilon_{210} = 4513 \text{ M}^{-1}\text{cm}^{-1}$. Stock solution of Oxaliplatin was found 13000 μM . More diluted solutions of Oxaliplatin were prepared with distilled water.

2.2.3 Synthesis of AuNPs and Modification of the Working Electrode

AuNPs were synthesized with minor modifications according to the citrate reduction method described by Turkevich et al. [102]. In short, 0.0984 g of $\text{HAuCl}_4 \cdot \text{H}_2\text{O}$ (purchased from Sigma-Aldrich, St. Louis, MO, USA) was dissolved with 500 mL of Millipore water to get 0.5 mM HAuCl_4 . After the solution was refluxed, 50.0 mL of 38.8 mM $\text{Na}_3\text{C}_6\text{H}_5\text{O}_7 \cdot 2\text{H}_2\text{O}$ solution (Sigma-Aldrich) was added in it with

vigorous stirring. Observed colors were pale yellow, colorless, and dark violet, respectively. The mixture was boiled with stirring for an additional 20 minutes to complete the synthesis of citrate capped AuNPs reaction by observing wine red color. The synthesized AuNPs solution was cooled to the room temperature and kept in the dark at 4°C overnight. Before characterization and detection experiments, stock solution of synthesized and purified AuNPs was diluted with Millipore water by setting the maximum absorbance of the prepared AuNPs solution to 1.17 (SPR at 521 nm). By using the previously published molar extinction coefficient (ϵ_{521}) of $2.70 \times 10^8 \text{ M}^{-1} \text{ cm}^{-1}$, predicted concentration of AuNPs in suspension was 3.33 nM [103].

For preparation of electrochemical measurements, bare graphite electrode was cleaned and polished with emery paper and washed with distilled water for 5 seconds. After graphite electrode was dried, AuNPs were immobilized by pipetting 10.0 μL of solution and the electrode was let to dry for 1 hour.

2.2.4 Electrochemical Studies

For the electrochemical measurements, all experiments were performed in a cell containing 50.0 mM acetate buffer solution (pH 4.8) at room temperature unless otherwise specified. Before each measurement, the cell was purged with nitrogen for 5 minutes to remove oxygen completely from the cell. Pu22 G4 DNA and Oxaliplatin incubation samples were prepared by depositing 10.0 μL of Pu22 G4 DNA-Oxaliplatin solution that is previously incubated at 37°C for 3 hours onto the AuNPs modified graphite electrode's surface. The graphite electrode was also left at the room temperature for 1 h for drying. The unbound DNA from the electrode surface was removed by rinsing the electrode with acetate buffer solution for 5 seconds. Differential pulse voltammograms (DPVs) were recorded in the potential range of 0.40 V and 1.40 V at a pulse amplitude of 50.0 mV in 50.0 mM acetate buffer solution (pH 4.8). Three measurements were carried out in each cell using freshly

cleaned and AuNPs modified electrodes. The construction of the biosensor was represented schematically in Figure 2.1.

2.2.4.1 Optimization of the Amount of AuNPs Used in Modification of Graphite Electrode

First, AuNPs solution was diluted with varying amounts of distilled water (DW). 1:1 solution was prepared by diluting the AuNPs stock solution with an equal volume of distilled water. 1:2 solution was prepared by diluting the AuNPs stock solution with twice the volume of distilled water. Likewise, 1:3 and 1:4 solutions were prepared by diluting with distilled water. Then, each AuNPs solution was immobilized onto graphite electrode surface which is left at room temperature for 1 h for drying. 10.0 μL of 10.0 μM Thiolated Pu22 G4 DNA solution was deposited onto each AuNPs modified graphite electrode's surface. The graphite electrode was also left at the room temperature for 1 h for drying. The unbound DNA from the electrode surface was removed by rinsing the electrode with acetate buffer solution for 5 seconds. All measurements were performed in a cell containing 50.0 mM acetate buffer solution (pH 4.8) at room temperature. Before each measurement, the cell was purged with nitrogen for 5 minutes to remove oxygen completely from the cell. Differential pulse voltammograms (DPVs) were recorded in the potential range of 0.40 V and 1.40 V at a pulse amplitude of 50.0 mV in 50.0 mM acetate buffer solution (pH 4.8).

2.2.4.2 Optimization of Pu22 G4 DNA Concentration on the Graphite Electrode

0.5 μM , 0.75 μM , 1.0 μM , 2.0 μM , 3.0 μM , 5.0 μM , 10.0 μM and 20.0 μM DNA solutions were prepared by diluting the stock solution of 36.8 μM Thiolated Pu22 G4 DNA with 50.0 mM acetate buffer (pH 4.8) containing 0.02 M NaCl. 10.0 μL of varying concentrations of Thiolated Pu22 G4 DNA solution was deposited onto each AuNPs modified graphite electrode's surface. The graphite electrode was left at the

room temperature for 1 h for drying. The unbound DNA from the electrode surface was removed by rinsing the electrode with acetate buffer solution for 5 seconds. All measurements were performed in a cell containing 50.0 mM acetate buffer solution (pH 4.8) at room temperature. Before each measurement, the cell was purged with nitrogen for 5 minutes to remove oxygen completely from the cell. Differential pulse voltammograms (DPVs) were recorded in the potential range of 0.40 V and 1.40 V at a pulse amplitude of 50.0 mV in 50.0 mM acetate buffer solution (pH 4.8). Three measurements were carried out in each cell using freshly cleaned and AuNPs modified electrodes.

2.2.4.3 Optimization of Incubation Time for Thiolated Pu22 G4 DNA and Oxaliplatin

To determine the effect of incubation time, equal volumes of 1.0 μM DNA was incubated with 1.0 μM Oxaliplatin for 30 min, 60 min, 90 min, 180 min and 24 hours. All incubations were performed at 37°C which is around body temperature. Pu22 G4 DNA and Oxaliplatin incubation samples were prepared by depositing 10.0 μL of Pu22 G4 DNA-Oxaliplatin solution that is previously incubated at 37°C for varying times onto the AuNPs modified graphite electrode's surface. The graphite electrode was also left at the room temperature for 1 h for drying. The unbound DNA from the electrode's surface was removed by rinsing the electrode with acetate buffer solution for 5 seconds. All measurements were performed in a cell containing 50.0 mM acetate buffer solution (pH 4.8) at room temperature. Before each measurement, the cell was purged with nitrogen for 5 minutes to remove oxygen completely from the cell. Differential pulse voltammograms (DPVs) were recorded in the potential range of 0.40 V and 1.40 V at a pulse amplitude of 50.0 mV in 50.0 mM acetate buffer solution (pH 4.8). Three measurements were carried out in each cell using freshly cleaned and AuNPs modified electrodes.

2.2.4.4 Optimization of Oxaliplatin Amount

First, 0.1 μM , 0.25 μM , 0.5 μM , 0.75 μM , 1.0 μM , 2.0 μM , 3.0 μM , 4.0 μM , 5.0 μM , 6.0 μM , 7.0 μM , 8.0 μM , 9.0 μM and 10.0 μM Oxaliplatin solutions were prepared by diluting the stock solution of 13000 μM Oxaliplatin with distilled water. Equal volumes of 1.0 μM DNA was incubated with varying concentrations of Oxaliplatin for 3 hours. All incubations were performed at 37°C which is around body temperature. Pu22 G4 DNA and Oxaliplatin incubation samples were prepared by depositing 10.0 μL of Pu22 G4 DNA-Oxaliplatin solution that is previously incubated at 37°C for varying times onto the AuNPs modified graphite electrode's surface. The graphite electrode was also left at the room temperature for 1 h for drying. The unbound DNA from the electrode surface was removed by rinsing the electrode with acetate buffer solution for 5 seconds. All measurements were performed in a cell containing 50.0 mM acetate buffer solution (pH 4.8) at room temperature. Before each measurement, the cell was purged with nitrogen for 5 minutes to remove oxygen completely from the cell. Differential pulse voltammograms (DPVs) were recorded in the potential range of 0.40 V and 1.40 V at a pulse amplitude of 50.0 mV in 50.0 mM acetate buffer solution (pH 4.8). Three measurements were carried out in each cell using freshly cleaned and AuNPs modified electrodes.

2.2.4.5 Surface Morphologies

For the surface morphology of the electrodes, bare graphite electrode, AuNPs modified graphite electrode, immobilized Pu22 G4 DNA onto AuNPs modified graphite electrode, and immobilized Pu22 G4 DNA and Oxaliplatin incubation sample onto AuNPs modified graphite electrode were prepared. Under selected optimum conditions, 10.0 μL of 1:2 AuNPs solution, 10.0 μL of 1.0 μM Pu22 G4 DNA, and 10.0 μL of 1.0 μM Oxaliplatin were used to prepare the electrodes for the

surface characterization. The surface morphology of the electrode at each step was monitored by Scanning Electron Microscopy (SEM) with different scales.

2.2.5 Circular Dichroism Fluorescence Spectroscopy Studies

For the Circular Dichroism (CD) and fluorometric measurements, varying concentration ratios of Pu22 G4 DNA:Oxp samples were prepared. Measurements were performed with Pu22 G4 DNA:Oxp samples with the concentration ratios of 1:0, 1:1, 1:5, 3:0, 3:3, 3:15, and 0:3. 1:0 represents that there is 1.0 μM Pu22 G4 DNA and no Oxaliplatin in the solution. 1:1 represents that there is equal volume of 1.0 μM Pu22 G4 DNA and 1.0 μM Oxaliplatin in the solution. 0:1 represents that there is no Pu22 G4 DNA and 1.0 μM Oxaliplatin. CD spectra were collected between 200 nm and 400 nm, with a scanning speed of 200 nm/min and 2 seconds integration time. Thioflavin T (ThT) was added in each solution at a final concentration of 1.0 μM for the fluorometric measurements. Emission spectra were collected between 430 nm and 700 nm excitation wavelength 420 nm with operation of 800 V.

2.2.6 Thermal Denaturation Studies

For the fluorometric measurements, varying concentration ratios of Pu22 G4 DNA:Oxp samples were prepared. Thermal denaturation experiments were performed with Pu22 G4 DNA:Oxp samples with the ratios of 3:0, 3:3, 3:15 (3 μM :0 μM , 3 μM :3 μM , 3 μM :15 μM) from 15°C to 95°C for heating and 95°C to 15°C for the cooling curves with 2°C using quartz cuvettes with PTFE stoppers (3.5 mL, 111-QS, Helma) in all spectrophotometric measurements. 3:0 represents that there is 3.0 μM Pu22 G4 DNA and no Oxaliplatin in the solution. 3:3 represents

that there is equal volume of 3.0 μM Pu22 G4 DNA and 3.0 μM Oxaliplatin in the solution. 3:15 represents that there is equal volume of 3.0 μM Pu22 G4 DNA and 15.0 μM Oxaliplatin in the solution. Absorbances were collected at 295 nm, and melting curves were plotted as normalized absorbance at 295 nm wavelength versus temperature lying between 15°C and 95°C.

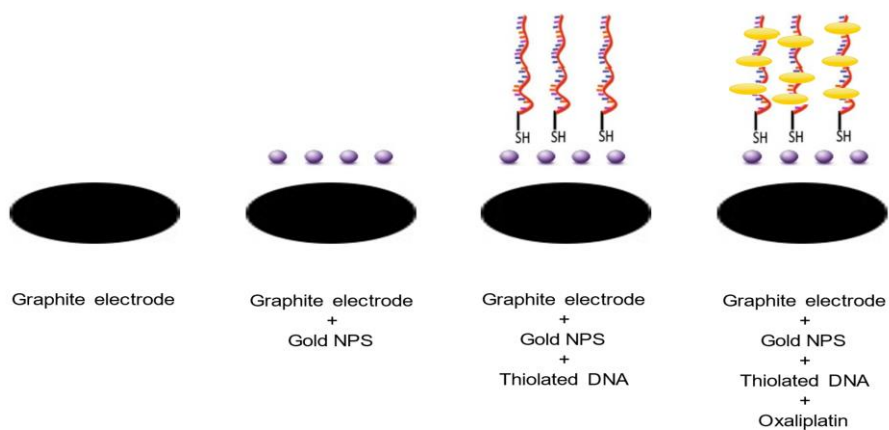


Figure 2.1. Schematic representation of AuNPs/Thiolated-DNA/GE construction

CHAPTER 3

RESULT AND DISCUSSION

3.1 Electrochemical Studies

With the discovery of the electroactivity of the bases in DNA, the identification and analysis of analytical biological materials via electrochemical methods has begun [104]. In this context, the detection of many analytes such as drugs, toxic substances, chemical warfare agents were carried out by utilizing their interactions with DNA [105]. Today, biosensor design based on DNA- analyte interactions is of great importance in finding new molecules in drug design and determining the interaction of these compounds with biochemical targets [106]. Studies with DNA biosensors provide us with important information in elucidating the structures of substances (for example, whether they have drug properties or not and the extent of their side effects) [107].

The interactions of the anticancer agent Oxaliplatin with Pu22 G4 DNA were investigated in this thesis using graphite electrode (GE) with gold nanoparticle (AuNPs) modification and DPV as an electrochemical method.

The suggested AuNPs modified biosensor was optimized for AuNPs' concentration, DNA concentration, incubation time, and Oxaliplatin amount by using differential pulse voltammetry response between 0.40 V and 1.40 V.

In the DPV technique, the oxidation of the electroactive guanine base in DNA is accepted as a signal [108]. The guanine base is oxidized around 0.8 V and responds with a certain current. When DNA interacts with Oxaliplatin, which is a cancer agent, it creates a crosslink with the guanine base in DNA and prevents guanine oxidation. As a result, a decrease in the guanine oxidation signal is expected. Özsöz et al., using the DPV technique, conducted the damage caused by arsenic, one of the heavy

metals, on DNA. In the determination of damage, the current given by guanine oxidation was observed in the presence and absence of arsenic, and it was concluded that there was a decrease in the guanine oxidation current in damaged DNA in the presence of arsenic [109]. Similarly, the decrease in the guanine oxidation signal was used by Yardim et al. to determine the DNA damage occurred in dsDNA by Cisplatin [110].

3.1.1 Optimization of the Amount of AuNPs Used in Modification of Graphite Electrode

AuNPs is mostly used for modification of electrodes in electrochemical DNA studies to increase DNA immobilization on the electrode's surface since especially Thiolated DNA structures are known to have strong affinity to gold [111], [112], [113]. In addition, AuNPs was especially preferred in modification of graphite electrodes since it increases the surface area of the electrode and enhances the electrical conductivity of the biosensor [111]. Khater et al. detected plant virus by electrochemical methods. In their study, they found that by modifying the screen-printed electrode with gold nanoparticles, the gold nanoparticle increased the peak intensity, that is, increased the electrical conductivity [114]. In another study, Liu et al. used AuNPs for surface modification of Thiolated DNA biosensor. Detection of target DNA was performed with bare and AuNPs modified electrode which was concluded that there was an increase of the detected amount of DNA with the sensitivity enhancement [115]. In another study, sensitive DNA biosensors based on gold nanoparticles were performed to show the damage caused by Cd(II) ions on DNA. With this sensor, DNA damage caused by Cd²⁺ ions were detected by measuring the peak current in differential pulse voltammetry. The gold nanoparticles were exploited to increase the signal by amplifying the current [116]. In this thesis, AuNPs was used for modification of GE with the expectation that it would increase electrical conductivity, create a good attachment bed for thiolated DNA, and increase the electrode surface area to enhance immobilization of thiolated DNA.

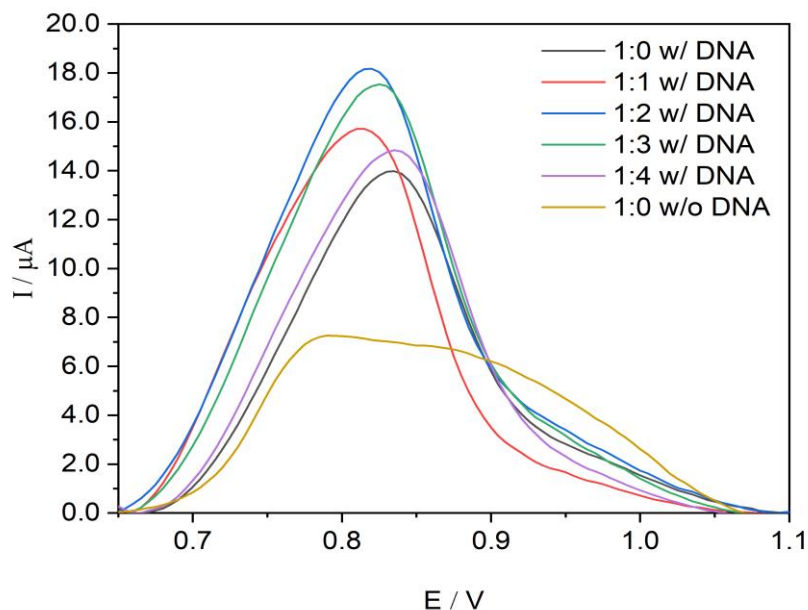


Figure 3.1. Differential pulse voltammograms (DPV) of 10.0 μM Pu22 G4 DNA on the graphite electrode coated with varying concentrations of AuNPs. 1:0 w/o DNA sample represents the bare GE electrode with no DNA and 1:1, 1:2, 1:3, 1:4 represents the samples with decreasing AuNP concentration. All the samples had 10.0 μM Thiolated Pu22 G4 DNA except 1:0 w/o DNA sample.

To observe the effect of AuNPs concentration on the response of the biosensor, AuNPs diluted to varied concentrations, ratios of 1:0, 1:1, 1:2, 1:3, 1:4 (AuNPs: Distilled Water), were used to modify the graphite electrode. As seen in Figure 3.1., using AuNPs on GE surface compared to the bare electrode, was proven to increase the effective electrode surface area, thereby increasing the electron transfer rate, with a slight increase in voltametric response of 10.0 μM Thiolated Pu22 G4 DNA. However, the use of higher concentrations of AuNPs clearly reduced the peak current as observed in Figure 3.1., which may be reasonable considering that electron transfer of DNA to the underlying electrode surface is partially blocked due to AuNPs saturation [117]. The highest signal was obtained for the sample where the AuNPs were diluted in 1:2 ratio (Figure 3.1.) which was used for further experiments.

3.1.2 Optimization of Pu22 G4 DNA Concentration on the Graphite Electrode

Next, the effect of DNA concentration on the response of the sensor was investigated via measuring DPV of AuNP coated electrode in the presence of varying concentrations of Pu22 G4 DNA (between 0.5 μM and 20.0 μM). Our goal in DNA concentration optimization was to determine a feasible DNA concentration that will give rise to decent signal, that can be used in further experiments to track the guanine oxidation by Oxaliplatin. As displayed in Figure 3.2., even though it wasn't a linear relationship, DPV signal was observed to be increasing with increasing DNA concentration. Liu et al. conducted a study to determine the damage caused by Mycobacterium tuberculosis on DNA by electrochemical methods. In their work, they developed a DNA biosensor using glassy carbon electrode. In the study, they observed a similar increase in peak intensity with increasing DNA concentration during DNA optimization. However, they concluded that this increase is not linear since excess DNA blocks electron transfer by causing saturation [118]. The change in DPV signal was more apparent when maximum current (I) was plotted against DNA concentration as displayed in Figure 3.3. Since the signal was relatively high at 1.0 μM DNA concentration, 1.0 μM DNA concentration was chosen as the concentration to be used in further experiments. The lower DNA concentration was selected also to demonstrate the applicability of the probe in detection of DNA damage even at low DNA concentrations and prevent the excess consumption of DNA.

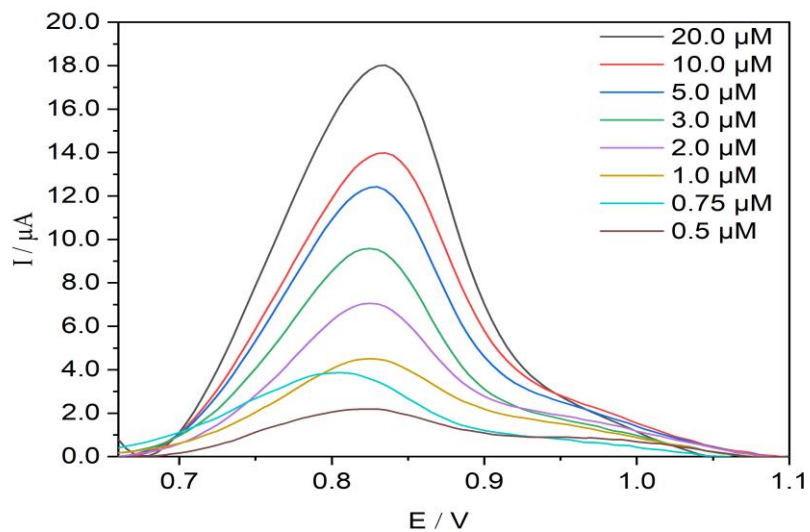


Figure 3.2. Differential pulse voltammograms (DPV) of Pu22 G4 DNA at varying DNA concentrations (between 0.5 and 20.0 μM). Three measurements were carried out in each cell using freshly cleaned and AuNPs modified electrodes

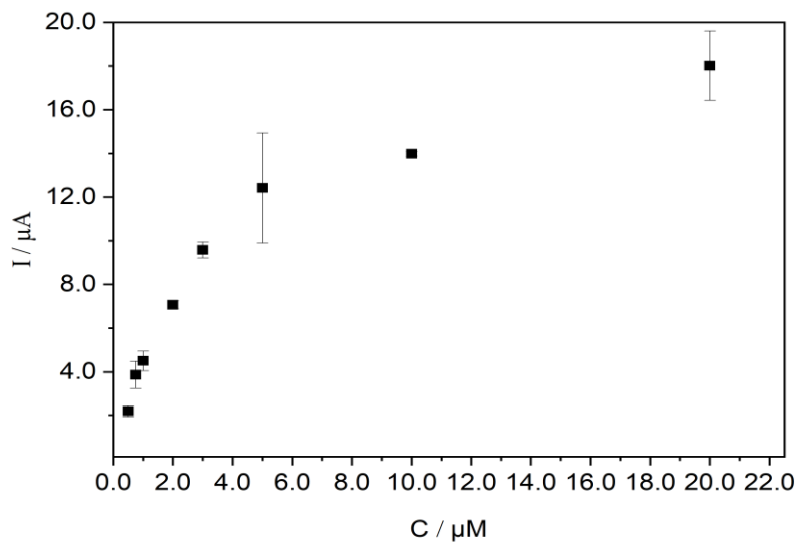


Figure 3.3. Differential pulse voltammograms (DPV) of Pu22 G4 DNA at varying concentrations

3.1.3 Optimization of Incubation Time for Pu22 G4 DNA and Oxaliplatin

Previous studies have shown that incubation time has an effect of the damage induced by Cisplatin on DNA. Jantarat et al. developed a label free fluorescent DNA sensor for the detection of Cisplatin induced G-Quadruplex DNA damage [119]. They also performed incubation time optimization for G-Quadruplex DNA and Cisplatin interaction. Looking at the graph of fluorescence intensity and the incubation time varying between 1 and 3 hours, they concluded that the 2.5 hour incubation time was optimum because the plateau was reached after 2.5 hours. In another study, Galagedera et al. developed an electrochemical sensor for detection of the level of dsDNA cross-linking with Cisplatin using a gold electrode. Likewise, the optimum interaction time of DNA and Cisplatin was determined, and it was found to be 18 hours [120]. Since the variation in the interaction time is related to the formation of different adducts, the factors affecting it are many such as DNA and drug type. As it can be understood, incubation time optimization is of great importance must be determined under the conditions investigated. After the optimization of AuNPs and DNA concentrations, the effect of varying incubation time on the response of the probe was examined at 37 °C. 37 °C of incubation temperature was preferred since it is taken as the body temperature and preferred also in many previous studies. For instance, Zhao et al. developed a fluorescent sensor for platinum drugs-DNA interactions based on quantum dots. They used Cisplatin as a platinum drug and interacted with DNA at 37 °C [121]. Kostrohunova et al. carried out studies on the different features of the DNA binding mode of Cisplatin. As incubation temperature of Cisplatin and DNA in all studies, they prefer 37 °C, which is body temperature [122]. Therefore, 37 °C of incubation temperature was preferred in this thesis study as it is body temperature. To determine the effect of incubation time, 1.0 μ M DNA was incubated with 1.0 μ M Oxaliplatin for 30 min, 60 min, 90 min, 180 min and 24 hours at 37°C.

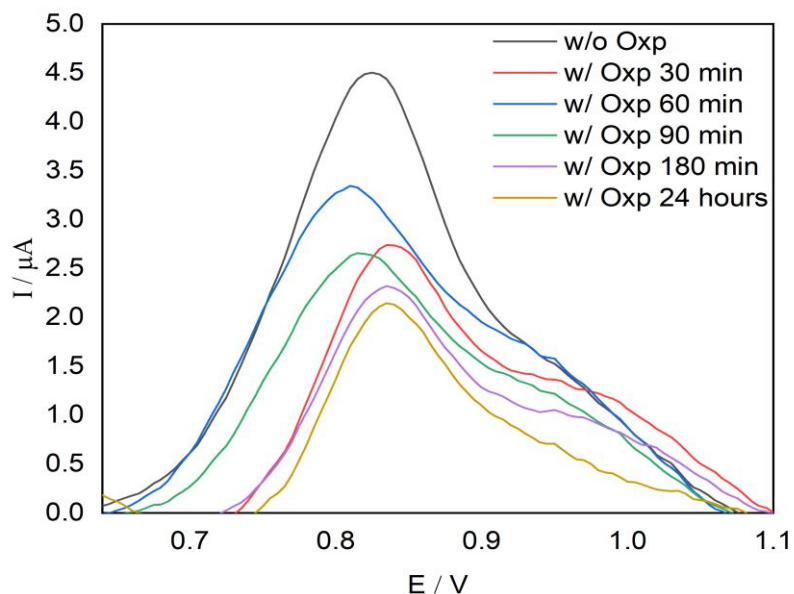


Figure 3.4. Differential pulse voltammograms (DPV) of 1.0 μM Pu22 G4 DNA incubated for varying time periods with 1.0 μM Oxaliplatin

As displayed in Figure 3.4, the DPV signal was decreased in the presence of Oxaliplatin. This decrease was taken as a sign of DNA damage. For instance, Topkaya et al., performed an electrochemical biosensor study for the damage caused by Irinotecan on DNA. In this study, using the differential pulse method, the decrease in guanine oxidation peak which indicates the damage caused by Irinotecan on DNA were shown [91]. The current of the 1.0 μM DNA without Oxaliplatin is 4.5 μA . The value was decreased to 3.3 μA when it was incubated for 60 minutes, 2.7 μA when it was incubated for 90 minutes, 2.3 μA when it was incubated for 3 hours and, 2.1 μA when it was incubated for 24 hours. Since the decrease was not significant for samples incubated for 3 and 24 hours, 3 hours incubation time was chosen as the incubation time to be used in the further experiments.

3.1.4 Optimization of Oxaliplatin Amount

Subsequently, the sensor to detect DNA damage induced by Oxaliplatin was developed under the optimized conditions. DPV signals of 1.0 μM DNA in the presence of varying concentrations of Oxaliplatin, between 0.1 μM and 10.0 μM , were measured in triplicates (Figure 3.5. & Figure 3.6.). The analytical merits of the sensor were obtained by using the DPV intensity at the maximum I of the guanine oxidation peak.

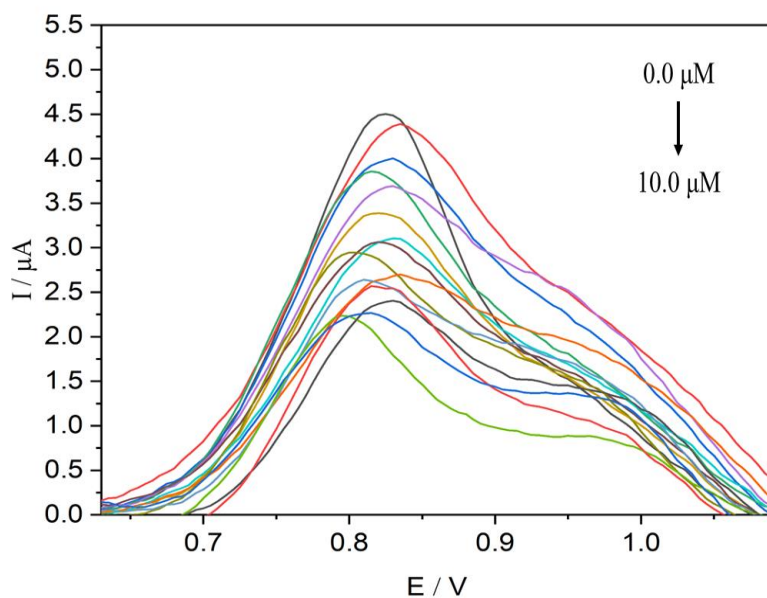


Figure 3.5. Differential pulse voltammograms (DPV) of 1.0 μM Pu22 G4 DNA in the presence of varying concentrations of Oxaliplatin

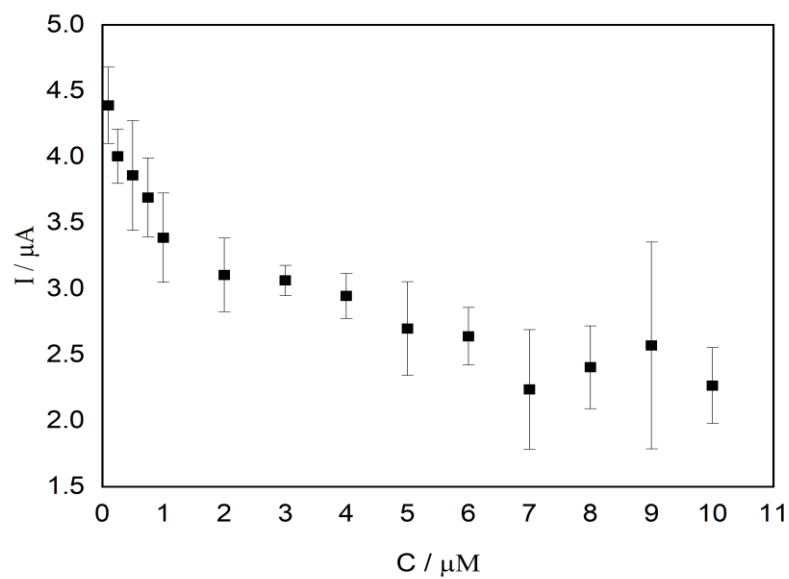


Figure 3.6. Differential pulse voltammograms (DPV) of 1.0 μM Pu22 G4 DNA in the presence of varying concentrations of Oxaliplatin

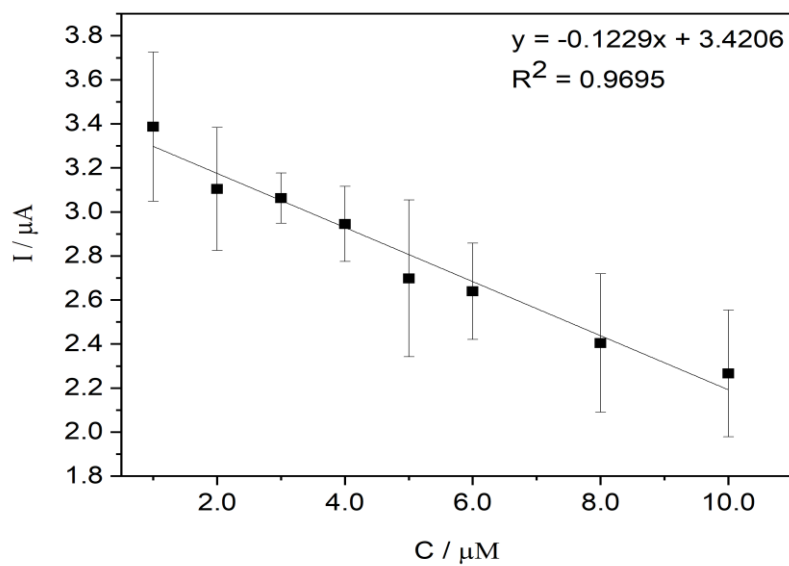


Figure 3.7. Calibration curve of 1.0 μM Pu22 G4 DNA in the presence of varying concentrations of Oxaliplatin

According to the data obtained, it was observed that the current was decreased as the Oxaliplatin concentration was increased. Based on these data, it can be concluded that as the covalent cross-linking of Oxaliplatin with DNA increases with increasing drug concentrations, the DNA structure is further deteriorated, and the guanine oxidation current decreases. Yardim et al. developed an electrochemical biosensor using graphene oxide modified glassy carbon electrode to demonstrate the damage Cisplatin causes on dsDNA [92]. In this study, which was carried out using the differential pulse method, 81% decrease in the guanine oxidation peak and the damage caused by Cisplatin on dsDNA were observed. As similar with our study, the current decrease in the signal was explained that as the Cisplatin concentration increases, crosslinking increases and thus DNA damage increases.

Under the optimized conditions, we were able to detect Oxaliplatin induced damage clearly at 1.0 μM Oxaliplatin concentration. Wekil et al. determined the damage caused by Oxaliplatin on ssDNA by DPV method using GCE and obtained 60 pmolL^{-1} limit of detection within 0.1-170 nmolL^{-1} range [123]. As stated, there are no studies conducted with Oxaliplatin with G-quadruplex and to our knowledge this is the first damage detection platform reported for a G-quadruplex structure and Oxaliplatin.

3.1.5 Surface Morphologies

The surface morphology of the electrode at each step was monitored by SEM. SEM images of bare graphite electrode and AuNPs modified graphite electrode are shown in Figure 3.8. The bare graphite's surface was relatively smooth before modification. The surface morphology of the bare graphite electrode was altered after AuNPs modification, where AuNPs immobilized on the graphite electrode surface exhibited a homogeneous dispersion. Aziz et al. modified the graphite pencil electrode with gold nanoparticle for high-sensitivity detection of hydrazine and found similar changes in the surface morphology of the electrode as our surface morphology [124]. Addition of Oxaliplatin onto AuNPs modified electrode altered the surface

morphology further where the crystal or rod like structures were observed. (Figure 3.9).

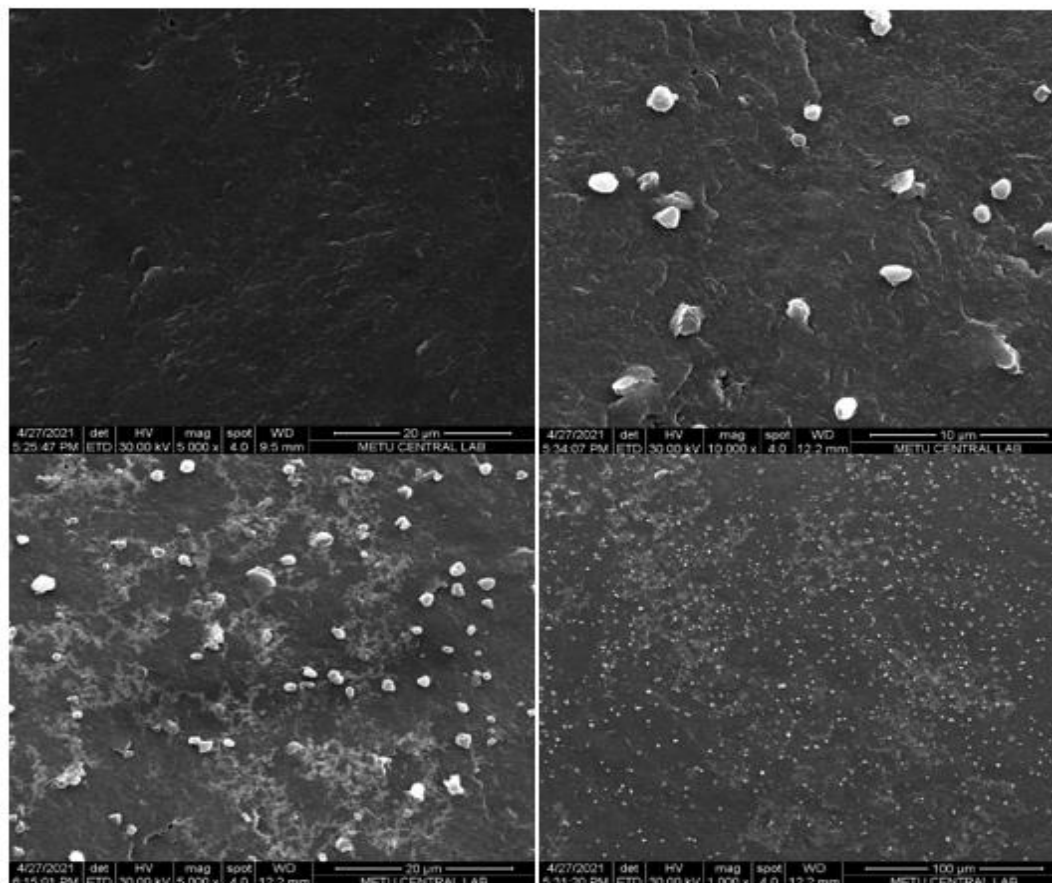


Figure 3.8. SEM images of bare graphite electrode and AuNPs modified surfaces under optimized conditions with different scales

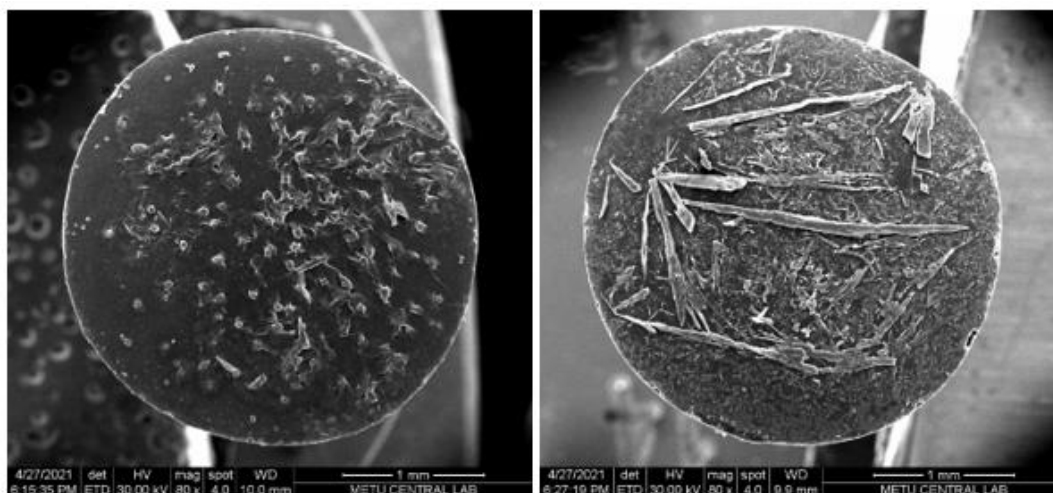


Figure 3.9. SEM images belonging to DNA on the electrode in the absence and presence of Oxaliplatin

3.2 Fluorometric Studies

Fluorescence spectroscopy is one of the most widely used techniques to study the interactions between small ligand molecules and DNA. Investigation of the interactions of Oxaliplatin with Pu22 G4 DNA using Thioflavin T (ThT) as a fluorescent probe. ThT alone is not fluorescent but becomes fluorescent in the presence of G-quadruplex [125], [126]. Zhang et al. developed a ThT induced G-quadruplex fluorescent biosensor for target DNA detection [126]. Fluorescence spectra were recorded with ThT excitation at a wavelength of 425 nm in the wavelength range of 450 to 600 nm. There is a marked increase in fluorescence intensity, with the maximum fluorescence peak occurring at 490 nm. On the other hand, in another study, it has been shown that the fluorescence intensity does not increase much when bound to single or double-stranded DNA, therefore ThT is used to detect G-quadruplex structures and the molecules that bind to these structures [127]. If the signal is high, there is a G-quadruplex structure and ThT is interacting with this structure, and we thought that if the signal was decreased, it would indicate a change in the G-quadruplex structure or binding.

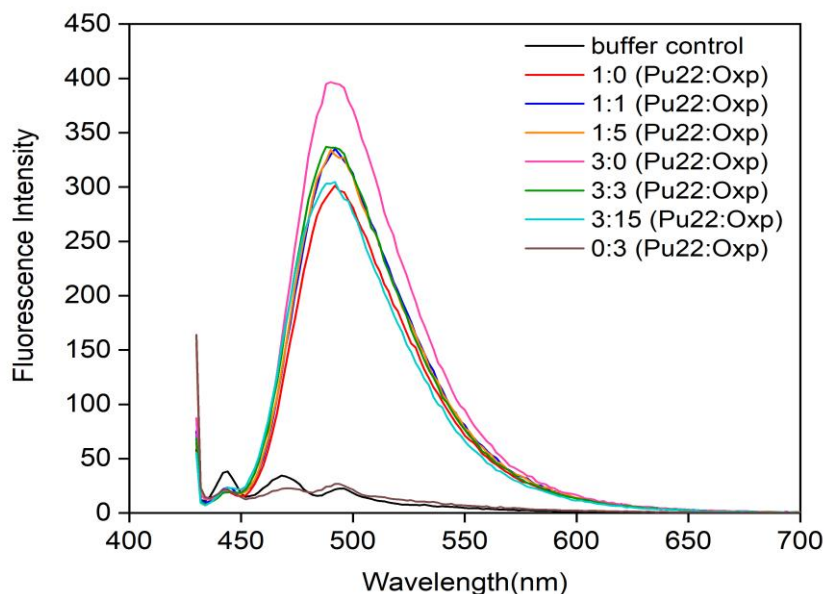


Figure 3.10. Fluorescence Spectroscopy of varying molarity ratios of Pu22 G4 DNA:Oxp

Fluorescence measurements were performed with Pu22 G4 DNA:Oxp samples with the molarity ratios of 1:0, 1:1, 1:5, 3:0, 3:3, 3:15, and 0:3. Emission spectra were collected between 430 nm and 700 nm with operation of 800 V. From Figure 3.10, the fluorescence intensity was decreased by adding Oxaliplatin. This result might be an indication of the structural disruption of Pu22 G4 DNA upon Oxaliplatin interaction.

3.3 Thermal Denaturation Studies

Thermal denaturation, with spectroscopic detection, offers one tried and true approach for measuring the stability of nucleic acid structures. The stability of G-quadruplexes is generally determined by observing the change in absorbance at 295

nm in UV [128]. In addition, the effects of ligands that bind to DNA on DNA can be determined by looking at the changes in thermal denaturation profiles [129].

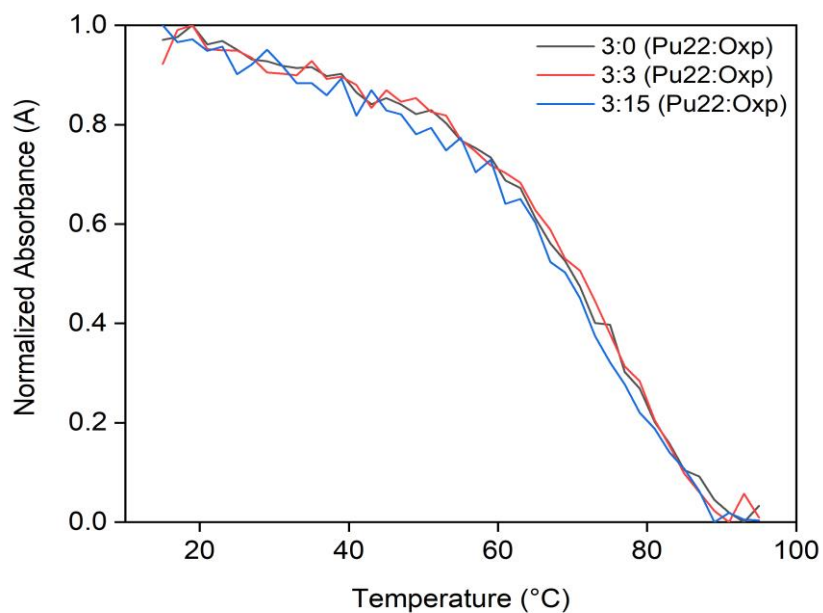


Figure 3.11. Heating curve of varying molarity ratios of Pu22 G4 DNA:Oxp

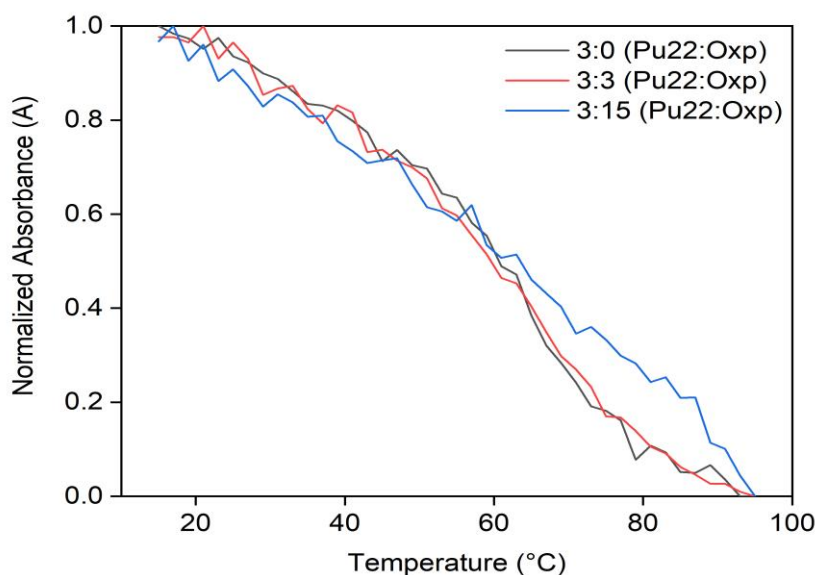


Figure 3.12. Cooling curve of varying molarity ratios of Pu22 G4 DNA:Oxp

Thermal denaturation experiments were performed with Pu22 G4 DNA:Oxp samples with the ratios of 3:0, 3:3, 3:15 at the temperature beginning from 15°C to 95°C for heating and vice versa for cooling curves with 2°C rate. Absorbances were collected at 295 nm, and melting curves were plotted as normalized absorbance at 295 nm wavelength versus temperature lying between 15°C and 95°C. The T_m was determined to be as 69 °C from the mid-points of the thermal denaturation profiles. However, no change in the melting profile was observed upon addition of Oxaliplatin to Pu22. This is contrary to our expectations, and it will be investigated further in future studies.

3.4 Circular Dichroism Studies

Circular dichroism (CD) spectra of the samples were also measured to observe if the presence of Oxaliplatin resulted in any structural changes in Pu22 G4 DNA. CD experiments were performed with Pu22 G4 DNA:Oxp samples with the ratios of 1:0, 1:1, 1:5, 3:0, 3:3, 3:15, 0:3. CD is a widely used method to characterize the secondary structures of proteins and nucleic acids [130]. The G4 structures formed by Pu22 have been previously characterized in detailed NMR studies by Yang et al. and are known to form parallel G4s that exhibit characteristic bands in their CD spectra [131]. Parallel G4 structures characteristically show a positive band around 260 nm and a negative band around 240 nm in CD spectra [132].

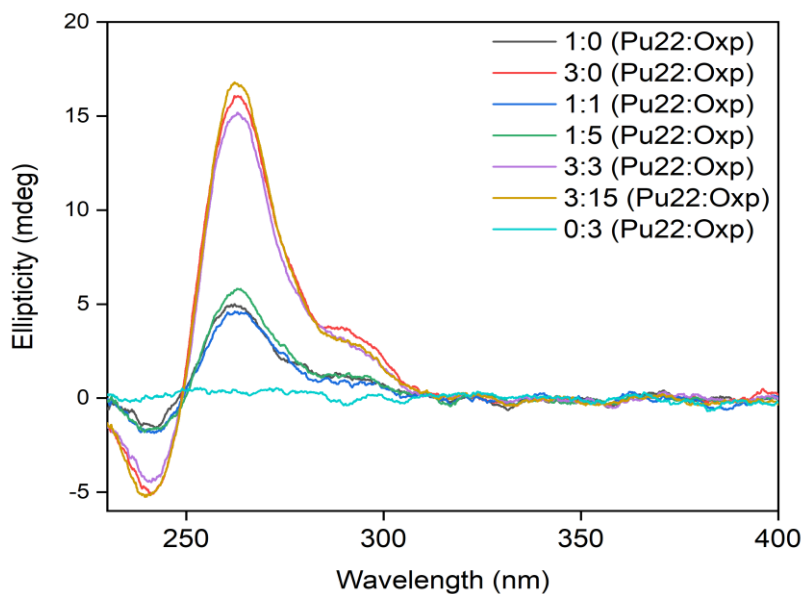


Figure 3.13. CD spectra of varying molarity ratios of Pu22 G4 DNA:Oxp

In addition to the positive band around 260 nm and a negative band around 240 nm, a small band at 290 nm is observed in the samples, which is an indicator of the formation of a hybrid structure [133]. When the CD spectra of Pu22 in the presence and absence of Oxaliplatin was compared, no major structural change in the structure was observed. The CD profiles were very similar except slight changes in ellipticity values especially at 260 nm and 290 nm. This result is contrary to our expectations, and it will be investigated further in future studies.

CHAPTER 4

CONCLUSIONS

Oxaliplatin, is a platinum-based third generation anticancer agent. It is currently used in the treatment of the colorectal cancer, and it is evaluated in clinical trials for other cancer types. As mentioned above Oxaliplatin is known to form DNA adducts and inhibit DNA synthesis mainly by the formation of inter- or intra- crosslinking of N7 of adenine and guanine bases [74]. To understand the molecular mechanisms underlying the side effects of platinum-based drugs and the resistance that develops against them and, there is a need for rapid qualitative and quantitative determination of the damage caused by these drugs [82]. In this thesis, AuNPs modified graphite electrode biosensor was successfully fabricated for detection of Oxaliplatin damage on G-Quadruplex forming VEGF structure for the first time. The surface of the graphite electrode was modified with AuNPs for increased immobilization of the thiolated Pu22, thus for design of a more stable, and sensitive biosensor. DPV measurements were taken in the range of 0.4V to 1.4V in the ABS buffer. The oxidation signal of guanine was used to investigate the interactions between Oxaliplatin and Pu22 G4 DNA without using any redox indicator. It was determined that the electrochemical behavior of the electrodes improved in the presence of AuNPs. AuNPs are known to increase the electroactive surface area, the conductivity of the surface and the electron transfer rate [37], [38]. Different concentrations of Oxaliplatin were used for investigating the interactions Oxaliplatin with Pu22 G4 DNA. A decrease in the oxidation signal was observed with increasing Oxaliplatin concentration possibly due to the decrease in the oxidation of guanine bases in the presence of Oxaliplatin. Plausibly, the crosslinking of guanine bases by Oxaliplatin and the formation of DNA adducts decreased the oxidation of guanine bases [82], [91], [110]. The damage was observable even at very low concentrations of Oxaliplatin, 0.1 μM . Still, the linear range is determined to be between 1.0 μM and

10.0 μM Oxaliplatin concentration. The surface characterization of the prepared electrodes was also performed by scanning electron microscopy. SEM images clearly revealed the changes on the surface of the electrode upon addition of each component, AuNP, DNA and Oxaliplatin. Electrochemical DNA damage studies were supported by the fluorescence spectroscopy. ThT is known to give rise to fluorescence signal upon binding to G4 structures [125], [126]. There was a slight decrease in the fluorescence intensity upon addition of Oxaliplatin to Pu22+ThT samples. The decrease increased with increasing Oxaliplatin concentration supporting the electrochemical studies. On the other hand, to our surprise no change was observed in thermal denaturation temperature of Pu22 and second structure of Pu22 in the presence of Oxaliplatin. At this moment, it is not clear whether the structure of Pu22 is changing upon Oxaliplatin binding. This discrepancy and so the interactions of Pu22 with Oxaliplatin will be assessed in future studies.

Still, to our knowledge this is the first study in which the interactions of Oxaliplatin with Pu22 G4 were investigated and an electrochemical biosensor using graphite electrode was developed. We believe that our study will open up new avenues in understanding the interactions of platin based drugs with DNA especially with G4 DNA structures.

REFERENCES

- [1] J. Watson, F. C.- Nature, and undefined 1953, “Molecular structure of nucleic acids: a structure for deoxyribose nucleic acid,” *Nature*, vol. 171, pp. 737–738, 1953, Accessed: Jul. 06, 2022. [Online]. Available: <https://www.nature.com/articles/171737a0>.
- [2] S. A. QUARRIE, “Phillips, R.L. and Vasil, I.K. DNA-based markers in plants. 2nd edn.,” *Annals of Botany*, vol. 91, no. 6, p. 749, May 2003, doi: 10.1093/AOB/MCG078.
- [3] N. Chatterjee, G. W.-E. and molecular, and undefined 2017, “Mechanisms of DNA damage, repair, and mutagenesis,” *Wiley Online Library*, vol. 58, no. 5, pp. 235–263, Jun. 2017, doi: 10.1002/em.22087.
- [4] S. Zhang, G. Wright, Y. Yang.,and Bioelectronics, and undefined 2000, “Materials and techniques for electrochemical biosensor design and construction,” *Biosens Bioelectron*, vol. 15, 2019, doi:10.1016/s0956-5663(00)00076-2. PMID:11219739.
- [5] P. Coulet and L. Blum, “Biosensor principles and applications,” 2019, Accessed: Jun. 27, 2022. [Online]. Available: <https://www.google.com/books?hl=tr&lr=&id=Szj3DwAAQBAJ&oi=fnd&pg=PP1&dq=biosensor+principles+and+applications&ots=dcR5-qxAHV&sig=bijv5wd3AfgyjtVaXmqzTsiEbLI>
- [6] J. Wang, “Glucose Biosensors: 40 Years of Advances and Challenges,” *Electroanalysis*, vol. 13, no. 12, 2001, doi: 10.1002/1521-4109(200108)13:12.
- [7] V. K. Gupta, M. L. Yola, M. S. Qureshi, A. O. Solak, N. Atar, and Z. Üstündağ, “A novel impedimetric biosensor based on graphene oxide/gold

- nanoplatforM for detection of DNA arrays,” *Sensors and Actuators, B: Chemical*, vol. 188, pp. 1201–1211, 2013, doi: 10.1016/j.snb.2013.08.034.
- [8] A. J. Bard *et al.*, “The electrode/electrolyte interface - A status report,” *Journal of Physical Chemistry*, vol. 97, no. 28, pp. 7147–7173, 1993, doi: 10.1021/J100130A007.
- [9] D. A. Skoog, F. J. Holler, and S. R. Crouch, *Principles of Instrumental Analysis sixth edition-Brooks Cole*, vol. 152. 2006.
- [10] Ü. Demirbaş, D. Akyüz, H. T. Akçay, A. Koca, O. Bekircan, and H. Kantekin, “Electrochemical and spectroelectrochemical study on novel non-peripherally tetra 1,2,4-triazole substituted phthalocyanines,” *Journal of Molecular Structure*, vol. 1155, pp. 380–388, Mar. 2018, doi: 10.1016/J.MOLSTRUC.2017.10.115.
- [11] C. G. Zoski, “Handbook of electrochemistry,” *Handbook of Electrochemistry*, 2007, doi: 10.1016/B978-0-444-51958-0.X5000-9.
- [12] J. L. Gómez-Cámer and P. Novák, “Electrochemical impedance spectroscopy: Understanding the role of the reference electrode,” *Electrochemistry Communications*, vol. 34, pp. 208–210, 2013, doi: 10.1016/j.elecom.2013.06.016.
- [13] V. v. Pavlishchuk and A. W. Addison, “Conversion constants for redox potentials measured versus different reference electrodes in acetonitrile solutions at 25°C,” *Inorganica Chimica Acta*, vol. 298, no. 1, pp. 97–102, Jan. 2000, doi: 10.1016/S0020-1693(99)00407-7.
- [14] F. A. Settle, *Handbook of instrumental techniques for analytical chemistry*. Upper Saddle River NJ: Prentice Hall PTR, 1997.
- [15] F. Scholz, “Electroanalytical methods: Guide to experiments and applications,” *Electroanalytical Methods: Guide to Experiments and Applications*, pp. 1–359, 2010, doi: 10.1007/978-3-642-02915-8.

- [16] D. A. Skoog, D. M. West, and F. James. Holler, *Fundamentals of analytical chemistry*, 7th ed. Fort Worth: Saunders College Pub., 1996.
- [17] R. N. Adams, “Applications of Modern Electroanalytical Techniques to Pharmaceutical Chemistry,” *Journal of Pharmaceutical Sciences*, vol. 58, no. 10, pp. 1171–1184, Oct. 1969, doi: 10.1002/JPS.2600581002.
- [18] D. R. Thévenot, K. Toth, R. A. Durst, G. S. Wilson, and D. R. Thévenot, “Electrochemical biosensors: recommended definitions and classification,” 2001. [Online]. Available: www.elsevier.com/locate/bios
- [19] L. C. Clark and C. Lyons, “Electrode systems for continuous monitoring in cardiovascular surgery,” *Ann N Y Acad Sci*, vol. 102, no. 1, pp. 29–45, 1962, doi: 10.1111/J.1749-6632.1962.TB13623.X.
- [20] L. J. Blum and P. R. Coulet, “Biosensor Principles and Applications; Marcel Dekker, Inc; 1st edition, 1991,” doi: 10.4324/9780367810849.
- [21] J. Ferguson, T. Boles, C. Adams, D. W.-N. biotechnology, and undefined 1996, “A fiber-optic DNA biosensor microarray for the analysis of gene expression,” *nature.com*, Accessed: Jul. 06, 2022. [Online]. Available: <https://www.nature.com/articles/nbt1296-1681>
- [22] Ş. C. Cevher, S. A. Bekmezci, SaniyeSoylemez, Y. A. Udum, L. Toppare, and A. Çırpan, “Indenoquinoxalinone based conjugated polymer substrate for laccase biosensor,” *Materials Chemistry and Physics*, vol. 257, Jan. 2021, doi: 10.1016/j.matchemphys.2020.123788.
- [23] S. D. Jayasena, “Aptamers: An emerging class of molecules that rival antibodies in diagnostics,” *Clinical Chemistry*, vol. 45, no. 9, pp. 1628–1650, 1999, doi: 10.1093/clinchem/45.9.1628.
- [24] C. I. L. Justino, A. C. Freitas, R. Pereira, A. C. Duarte, and T. A. P. Rocha Santos, “Recent developments in recognition elements for chemical sensors

- and biosensors,” *TrAC - Trends in Analytical Chemistry*, vol. 68. Elsevier B.V., pp. 2–17, May 01, 2015. doi: 10.1016/j.trac.2015.03.006.
- [25] M. Badihi-Mossberg, V. Buchner, and J. Rishpon, “Electrochemical biosensors for pollutants in the environment,” *Electroanalysis*, vol. 19, no. 19–20. pp. 2015–2028, Oct. 2007. doi: 10.1002/elan.200703946.
- [26] M. C. Tran, “Biosensors (Sensor Physics and Technology Series),” 1993, Accessed: Jul. 06, 2022. [Online]. Available: <http://books.google.nl/books/about/Biosensors.html?id=HOkd68xeEiEC&pgis=1>
- [27] P. Mehrotra, “Biosensors and their applications – A review,” *Journal of Oral Biology and Craniofacial Research*, vol. 6, no. 2, pp. 153–159, May 2016, doi: 10.1016/J.JOBCR.2015.12.002.
- [28] V. Erduran, M. Bekmezci, R. Bayat, Z. B. Altuntaş, and F. Sen, “Functionalized nanomaterials and workplace health and safety,” *Functionalized Nanomaterial-Based Electrochemical Sensors: Principles, Fabrication Methods, and Applications*, pp. 393–406, Jan. 2022, doi: 10.1016/B978-0-12-823788-5.00015-6.
- [29] N. Bhalla, P. Jolly, N. Formisano, and P. Estrela, “Introduction to biosensors,” *Essays in Biochemistry*, vol. 60, no. 1, p. 1, Jun. 2016, doi: 10.1042/EBC20150001.
- [30] G. Fu, X. Yue, and Z. Dai, “Glucose biosensor based on covalent immobilization of enzyme in sol-gel composite film combined with Prussian blue/carbon nanotubes hybrid,” *Biosensors and Bioelectronics*, vol. 26, no. 9, pp. 3973–3976, May 2011, doi: 10.1016/j.bios.2011.03.007.
- [31] S. A. Bekmezci, S. Soylemez, G. Yilmaz, Y. A. Udum, Y. Yagci, and L. Toppare, “A new ethanol biosensor based on polyfluorene-g-poly(ethylene glycol) and multiwalled carbon nanotubes,” *European Polymer Journal*, vol. 122, Jan. 2020, doi: 10.1016/j.eurpolymj.2019.109300.

- [32] S. Singh *et al.*, “Biological Biosensors for Monitoring and Diagnosis,” pp. 317–335, 2020, doi: 10.1007/978-981-15-2817-0_14.
- [33] G. Liu and Y. Lin, “Nanomaterial labels in electrochemical immunosensors and immunoassays,” *Talanta*, vol. 74, no. 3. Elsevier, pp. 308–317, Dec. 15, 2007. doi: 10.1016/j.talanta.2007.10.014.
- [34] C. Jianrong, M. Yuqing, H. Nongyue, W. Xiaohua, and L. Sijiao, “Nanotechnology and biosensors,” *Biotechnology Advances*, vol. 22, no. 7, pp. 505–518, 2004, doi: 10.1016/j.biotechadv.2004.03.004.
- [35] B. Liu and J. Liu, “Methods for preparing DNA-functionalized gold nanoparticles, a key reagent of bioanalytical chemistry,” *Analytical Methods*, vol. 9, no. 18. Royal Society of Chemistry, pp. 2633–2643, May 14, 2017. doi: 10.1039/c7ay00368d.
- [36] Y. Li, H. J. Schluesener, and S. Xu, “Gold nanoparticle-based biosensors,” *Gold Bulletin*, vol. 43, no. 1, pp. 29–41, 2010, doi: 10.1007/BF03214964.
- [37] H. Cai, C. Xu, P. He, and Y. Fang, “Colloid Au-enhanced DNA immobilization for the electrochemical detection of sequence-specific DNA,” *Journal of Electroanalytical Chemistry*, vol. 510, no. 1–2, pp. 78–85, Sep. 2001, doi: 10.1016/S0022-0728(01)00548-4.
- [38] E. Heydari-Bafrooei, M. Amini, and S. Saeednia, “Electrochemical detection of DNA damage induced by Bleomycin in the presence of metal ions,” *Journal of Electroanalytical Chemistry*, vol. 803, pp. 104–110, Oct. 2017, doi: 10.1016/J.JELECHEM.2017.09.031.
- [39] P. Mehrotra, “Biosensors and their applications – A review,” *Journal of Oral Biology and Craniofacial Research*, vol. 6, no. 2, pp. 153–159, May 2016, doi: 10.1016/J.JOBCR.2015.12.002.
- [40] P. B. Dervan, “Sequence Specific Recognition of Double Helical DNA. A Synthetic Approach,” pp. 49–64, 1988, doi: 10.1007/978-3-642-83384-7_3.

- [41] I. P. Niclòs and J. G. García, “Beyond the double helix: The structure of DNA G-quadruplexes,” *Metode*, vol. 2022, no. 12, pp. 6–13, 2022, doi: 10.7203/METODE.12.16505.
- [42] B. X. Zheng *et al.*, “Rational design of Red fluorescent and selective G-quadruplex DNA sensing probes: The study of interaction signaling and the molecular structural relationship achieving high specificity,” *Sensors and Actuators, B: Chemical*, vol. 314, Jul. 2020, doi: 10.1016/j.snb.2020.128075.
- [43] A. de Rache, T. Doneux, and C. Buess-Herman, “Electrochemical discrimination between G-quadruplex and duplex DNA,” *Analytical Chemistry*, vol. 86, no. 16, pp. 8057–8065, Aug. 2014, doi: 10.1021/ac500791s.
- [44] S. Neidle, “Quadruplex Nucleic Acids as Novel Therapeutic Targets,” *Journal of Medicinal Chemistry*, vol. 59, no. 13. American Chemical Society, pp. 5987–6011, Jul. 14, 2016. doi: 10.1021/acs.jmedchem.5b01835.
- [45] A. Cammas and S. Millevoi, “RNA G-quadruplexes: emerging mechanisms in disease,” *Nucleic Acids Research*, vol. 45, no. 4, pp. 1584–1595, Feb. 2017, doi: 10.1093/NAR/GKW1280.
- [46] J. L. Huppert and S. Balasubramanian, “G-quadruplexes in promoters throughout the human genome,” *Nucleic Acids Research*, vol. 35, no. 2, pp. 406–413, Jan. 2007, doi: 10.1093/NAR/GKL1057.
- [47] M. Q. Wang *et al.*, “A benzo(f)quinolinium fused chromophore-based fluorescent probe for selective detection of c-myc G-Quadruplex DNA with a red emission and a large Stokes shift,” *Dyes and Pigments*, vol. 168, pp. 334–340, Sep. 2019, doi: 10.1016/J.DYEPIG.2019.05.004.
- [48] D. Sun *et al.*, “The proximal promoter region of the human vascular endothelial growth factor gene has a G-quadruplex structure that can be targeted by G-quadruplex-interactive agents,” *Mol Cancer Ther*, vol. 7, no. 4, pp. 880–889, 2008, doi: 10.1158/1535-7163.MCT-07-2119.

- [49] P. Agrawal, C. Lin, R. I. Mathad, M. Carver, and D. Yang, “The major G-quadruplex formed in the human BCL-2 proximal promoter adopts a parallel structure with a 13-nt loop in K⁺ solution,” *J Am Chem Soc*, vol. 136, no. 5, pp. 1750–1753, Feb. 2014, doi: 10.1021/ja4118945.
- [50] P. Agrawal, E. Hatzakis, K. Guo, M. Carver, and D. Yang, “Solution structure of the major G-quadruplex formed in the human VEGF promoter in K⁺: insights into loop interactions of the parallel G-quadruplexes,” *Nucleic Acids Research*, vol. 41, no. 22, pp. 10584–10592, Dec. 2013, doi: 10.1093/NAR/GKT784.
- [51] J. Folkman, “Role of angiogenesis in tumor growth and metastasis,” *Seminars in Oncology*, vol. 29, no. 6, pp. 15–18, Dec. 2002, doi: 10.1016/S0093-7754(02)70065-1.
- [52] D. C. Sullivan and R. Bicknell, “New molecular pathways in angiogenesis,” *British Journal of Cancer*, vol. 89, pp. 228–231, 2003, doi: 10.1038/sj.bjc.6601107.
- [53] M. Aita *et al.*, “Targeting the VEGF pathway: Antiangiogenic strategies in the treatment of non-small cell lung cancer,” *Critical Reviews in Oncology/Hematology*, vol. 68, no. 3, pp. 183–196, Dec. 2008, doi: 10.1016/J.CRITREVONC.2008.05.002.
- [54] D. Sun *et al.*, “The proximal promoter region of the human vascular endothelial growth factor gene has a G-quadruplex structure that can be targeted by G-quadruplex-interactive agents,” *Mol Cancer Ther*, vol. 7, no. 4, pp. 880–889, Apr. 2008, doi: 10.1158/1535-7163.MCT-07-2119.
- [55] M. H. Kaulage, B. Maji, S. Pasadi, A. Ali, S. Bhattacharya, and K. Muniyappa, “Targeting G-quadruplex DNA structures in the telomere and oncogene promoter regions by benzimidazole–carbazole ligands,” *European Journal of Medicinal Chemistry*, vol. 148, pp. 178–194, Mar. 2018, doi: 10.1016/J.EJMECH.2018.01.091.

- [56] R. de Bont and N. van Larebeke, "Endogenous DNA damage in humans: a review of quantitative data," *Mutagenesis*, vol. 19, no. 3, pp. 169–185, May 2004, doi: 10.1093/MUTAGE/GEH025.
- [57] G. Giglia-Mari, A. Zotter, and W. Vermeulen, "DNA damage response," *Cold Spring Harbor Perspectives in Biology*, vol. 3, no. 1, pp. 1–19, Jan. 2011, doi: 10.1101/cshperspect.a000745.
- [58] A. M. Oliveira-Brett, M. Vivan, I. R. Fernandes, and J. A. P. Piedade, "Electrochemical detection of in situ adriamycin oxidative damage to DNA," 2002. [Online]. Available: www.elsevier.com/locate/talanta
- [59] M. Fojta, "Electrochemical Sensors for DNA Interactions and Damage."
- [60] S. Steenken and S. v. Jovanovic, "How easily oxidizable is DNA? One-electron reduction potentials of adenosine and guanosine radicals in aqueous solution," *J Am Chem Soc*, vol. 119, no. 3, pp. 617–618, 1997, doi: 10.1021/JA962255B/ASSET/JA962255B.FP.PNG_V03.
- [61] S. Kawanishi, Y. Hiraku, and S. Oikawa, "Mechanism of guanine-specific DNA damage by oxidative stress and its role in carcinogenesis and aging," *Mutation Research - Reviews in Mutation Research*, vol. 488, no. 1, pp. 65–76, 2001, doi: 10.1016/S1383-5742(00)00059-4.
- [62] H. Kasai and Z. Yamaizumi, "Photosensitized Formation of 7,8-Dihydro-8-oxo-2'-deoxyguanosine (8-hydroxy-2'-deoxyguanosine) in DNA by Riboflavin: A Non Singlet Oxygen-Mediated Reaction," *J Am Chem Soc*, vol. 114, no. 24, pp. 9692–9694, Nov. 1992, doi: 10.1021/ja00050a078.
- [63] C. J. Burrows and J. G. Muller, "Oxidative Nucleobase Modifications Leading to Strand Scission," *Chemical Reviews*, vol. 98, no. 3, pp. 1109–1151, 1998, doi: 10.1021/CR960421S.
- [64] S. Chaney, A. S.-J. J. of the N. Cancer, and undefined 1996, "DNA repair: enzymatic mechanisms and relevance to drug response," *academic.oup.com*,

Accessed: Jul. 03, 2022. [Online]. Available:

<https://academic.oup.com/jnci/article-abstract/88/19/1346/991708>

- [65] N. Kondo, A. Takahashi, K. Ono, T. O.-J. of nucleic acids, and undefined 2010, “DNA damage induced by alkylating agents and repair pathways,” *hindawi.com*, Accessed: Jul. 03, 2022. [Online]. Available: <https://www.hindawi.com/journals/JNA/2010/543531/>
- [66] M. L. G. Dronkert and R. Kanaar, “Repair of DNA interstrand cross-links,” *Mutation Research/DNA Repair*, vol. 486, no. 4, pp. 217–247, Sep. 2001, doi: 10.1016/S0921-8777(01)00092-1.
- [67] Y. Huang and L. Li, “DNA crosslinking damage and cancer - a tale of friend and foe,” *Transl Cancer Res*, vol. 2, no. 3, pp. 144–154, Jun. 2013, doi: 10.3978/J.ISSN.2218-676X.2013.03.01.
- [68] J. Almagro, H. A. Messal, A. Elosegui-Artola, J. van Rheenen, and A. Behrens, “Tissue architecture in tumor initiation and progression,” *Trends in Cancer*, 2022, doi: 10.1016/J.TRECAN.2022.02.007.
- [69] E. C. Woodhouse, R. F. Chuaqui, L. A. Liotta, “General mechanisms of metastasis,” *Cancer*, vol. 80, pp. 1529–1566, 1997.
- [70] M. Sirajuddin, S. Ali, and A. Badshah, “Drug-DNA interactions and their study by UV-Visible, fluorescence spectroscopies and cyclic voltametry,” *Journal of Photochemistry and Photobiology B: Biology*, vol. 124, pp. 1–19, Jul. 05, 2013. doi: 10.1016/j.jphotobiol.2013.03.013.
- [71] T. W. Hambley, “The influence of structure on the activity and toxicity of Pt anti-cancer drugs,” *Coordination Chemistry Reviews*, vol. 166, pp. 181–223, 1997, doi: 10.1016/s0010-8545(97)00023-4.
- [72] “28-Platinum compounds a new class of potent antitumour agents”.

- [73] N. J. Wheate, S. Walker, G. E. Craig, and R. Oun, "The status of platinum anticancer drugs in the clinic and in clinical trials," *Dalton Transactions*, vol. 39, no. 35, pp. 8113–8127, Sep. 2010, doi: 10.1039/c0dt00292e.
- [74] F. Xiao, X. Luo, X. Fu, and Y. Zheng, "Cleavage enhancement of specific chemical bonds in DNA by cisplatin radiosensitization," *Journal of Physical Chemistry B*, vol. 117, no. 17, pp. 4893–4900, May 2013, doi: 10.1021/jp400852p.
- [75] B. Rosenberg, L. VanCamp, J. E. Trosko, and V. H. Mansour, "Platinum compounds: a new class of potent antitumour agents," *Nature*, vol. 222, no. 5191, pp. 385–386, 1969, doi: 10.1038/222385A0.
- [76] D. Wang and S. J. Lippard, "Cellular processing of platinum anticancer drugs," *Nature Reviews Drug Discovery*, vol. 4, no. 4, pp. 307–320, Apr. 2005. doi: 10.1038/nrd1691.
- [77] L. Kelland, "The resurgence of platinum-based cancer chemotherapy," *Nature Reviews Cancer*, vol. 7, no. 8, pp. 573–584, Aug. 19, 2007. doi: 10.1038/nrc2167.
- [78] M. D. Hall, M. Okabe, D. W. Shen, X. J. Liang, and M. M. Gottesman, "The role of cellular accumulation in determining sensitivity to platinum-based chemotherapy," *Annual Review of Pharmacology and Toxicology*, vol. 48, pp. 495–535, 2008. doi: 10.1146/annurev.pharmtox.48.080907.180426.
- [79] G. Los, P. H. A. Mutsaers, W. J. M. Lenglet, G. S. Baldew, and J. G. Mevie, "Platinum distribution in intraperitoneal tumors after intraperitoneal cisplatin treatment," *Cancer Chemother Pharmacol*, vol. 25, no. 6, 1990. doi: 10.1007/BF00686048. PMID: 2311166.
- [80] R. B. Weiss and M. C. Christian, "New Cisplatin Analogues in Development A Review," 1993.

- [81] S. Dilruba and G. v. Kalayda, "Platinum-based drugs: past, present and future," *Cancer Chemotherapy and Pharmacology*, vol. 77, no. 6. Springer Verlag, pp. 1103–1124, Jun. 01, 2016. doi: 10.1007/s00280-016-2976-z.
- [82] A. Yimit, O. Adebali, A. Sancar, and Y. Jiang, "Differential damage and repair of DNA-adducts induced by anti-cancer drug cisplatin across mouse organs," *Nature Communications*, vol. 10, no. 1, Dec. 2019, doi: 10.1038/s41467-019-08290-2.
- [83] R. Charif *et al.*, "Association of a Platinum Complex to a G-Quadruplex Ligand Enhances Telomere Disruption," *Chemical Research in Toxicology*, vol. 30, no. 8, pp. 1629–1640, Aug. 2017, doi: 10.1021/acs.chemrestox.7b00131.
- [84] Q. Cao, Y. Li, E. Freisinger, P. Z. Qin, R. K. O. Sigel, and Z. W. Mao, "G-quadruplex DNA targeted metal complexes acting as potential anticancer drugs," *Inorganic Chemistry Frontiers*, vol. 4, no. 1, pp. 10–32, Jan. 2017, doi: 10.1039/C6QI00300A.
- [85] I. Q. Garnier, R. Charif *et al.*, "Telomeres and telomerase: potential targets for platinum complexes," *Metal Complex-DNA Interactions*, vol. 4, 2009.
- [86] J. N. Burstyn, W. J. Heiger-Bernays, S. M. Cohen, and S. J. Lippard, "Formation of cis-diamminedichloroplatinum(II) 1,2-intrastrand cross-links on DNA is flanking-sequence independent," *Nucleic Acids Research*, vol. 28, no. 21, pp. 4237–4243, Nov. 2000, doi: 10.1093/NAR/28.21.4237.
- [87] S. Chuaychob *et al.*, "A nanobiosensor for the simple detection of small molecules using non-crosslinking aggregation of gold nanoparticles with G-quadruplexes," *Analytical Methods*, vol. 12, no. 3, pp. 230–238, Jan. 2020, doi: 10.1039/C9AY02150G.
- [88] R. Charif *et al.*, "Association of a Platinum Complex to a G-Quadruplex Ligand Enhances Telomere Disruption," *Chem Res Toxicol*, vol. 30, no. 8, pp. 1629–1640, Aug. 2017, doi: 10.1021/ACS.CHEMRESTOX.7B00131.

- [89] L. He, Z. Meng, D. Xu, and F. Shao, "Dual functional dinuclear platinum complex with selective reactivity towards c-myc G-quadruplex," *Scientific Reports* 2018 8:1, vol. 8, no. 1, pp. 1–9, Jan. 2018, doi: 10.1038/s41598-017-19095-y.
- [90] Z. Li, Y. Zilberman, Q. bin Lu, and X. Tang, "Electrochemical methods for probing DNA damage mechanisms and designing cisplatin-based combination chemotherapy," *Biotechniques*, vol. 66, no. 3, pp. 135–142, Mar. 2019, doi: 10.2144/btn-2018-0106 .
- [91] S. Nur Topkaya, S. Aydinlik, N. Aladag, M. Ozsoz, and D. Ozkan-Ariksoysal, "Different DNA immobilization strategies for the interaction of anticancer drug irinotecan with DNA based on electrochemical DNA biosensors," *Comb Chem High Throughput Screen*, vol. 13, no. 7, pp. 582–589, Nov. 2010, doi: 10.2174/1386207311004070582.
- [92] Y. Yardım, M. Vandeput, M. Çelebi, Z. Şentürk, and J. M. Kauffmann, "A Reduced Graphene Oxide-based Electrochemical DNA Biosensor for the Detection of Interaction between Cisplatin and DNA based on Guanine and Adenine Oxidation Signals," *Electroanalysis*, vol. 29, no. 5, pp. 1451–1458, May 2017, doi: 10.1002/ELAN.201600804.
- [93] A. J. Santiago-Lopez, J. L. Vera, and E. Meléndez, "DNA electrochemical biosensor for metallic drugs at physiological conditions," *Journal of Electroanalytical Chemistry*, vol. 731, pp. 139–144, Oct. 2014, doi: 10.1016/j.jelechem.2014.07.022.
- [94] M. Mascini, G. Bagni, M. L. di Pietro, M. Ravera, S. Baracco, and D. Osella, "Electrochemical biosensor evaluation of the interaction between DNA and metallo-drugs," *BioMetals*, vol. 19, no. 4, pp. 409–418, Aug. 2006, doi: 10.1007/s10534-005-4340-3.
- [95] H. Eda Satana Kara, "Redox mechanism of anticancer drug idarubicin and in-situ evaluation of interaction with DNA using an electrochemical

- biosensor,” *Bioelectrochemistry*, vol. 99, pp. 17–23, 2014, doi: 10.1016/j.bioelechem.2014.06.002.
- [96] E. E. S. Bruzaca, I. C. Lopes, E. H. C. Silva, P. A. v. Carvalho, and A. A. Tanaka, “Electrochemical oxidation of the antitumor antibiotic mitomycin C and in situ evaluation of its interaction with DNA using a DNA-electrochemical biosensor,” *Microchemical Journal*, vol. 133, pp. 81–89, Jul. 2017, doi: 10.1016/j.microc.2017.03.030.
- [97] S. K. K. Galagedera and G. U. Flechsig, “Detection of the level of DNA cross-linking with cisplatin by electrochemical quartz crystal microbalance,” *Journal of Electroanalytical Chemistry*, vol. 862, Apr. 2020, doi: 10.1016/j.jelechem.2020.113992.
- [98] A. M. Oliveira Brett, M. A. La-Scalea, S. H. P. Serrano, T. A. Macedo,+,’, D. Raimundo, and ’ M Helenu Marquesi, “Electrochemical Determination of Carboplatin in Serum Using a DNA-Modified Glassy Carbon Electrode,” *Electroanalysis*, vol. 8, no. 11, 1996, doi: 10.1002/elan.1140081104
- [99] B. Dogan-Topal and S. A. Ozkan, “Electrochemical determination of anticancer drug fulvestrant at dsDNA modified pencil graphite electrode,” *Electrochimica Acta*, vol. 56, no. 12, pp. 4433–4438, Apr. 2011, doi: 10.1016/j.electacta.2011.01.066.
- [100] P. Palaska, E. Arizoglou, and S. Girousi, “Sensitive detection of cyclophosphamide using DNA-modified carbon paste, pencil graphite and hanging mercury drop electrodes,” *Talanta*, vol. 72, no. 3, pp. 1199–1206, May 2007, doi: 10.1016/j.talanta.2007.01.013.
- [101] B. Dogan-Topal and S. A. Ozkan, “A novel sensitive electrochemical DNA biosensor for assaying of anticancer drug leuprolide and its adsorptive stripping voltammetric determination,” *Talanta*, vol. 83, no. 3, pp. 780–788, Jan. 2011, doi: 10.1016/j.talanta.2010.10.049.

- [102] J. Turkevich, P. C. Stevenson, and J. Hillier, "A study of the nucleation and growth processes in the synthesis of colloidal gold," *Discuss Faraday Soc.*, vol. 11, no. 0, pp. 55–75, Jan. 1951, doi: 10.1039/DF9511100055.
- [103] M. M. Maye *et al.*, "Gold and alloy nanoparticles in solution and thin film assembly: spectrophotometric determination of molar absorptivity," *Analytica Chimica Acta*, vol. 496, no. 1–2, pp. 17–27, Oct. 2003, doi: 10.1016/S0003-2670(03)00986-3.
- [104] E. Palecek *et al.* "Electrochemistry of Nucleic Acids and Non-Conjugated Proteins." *American Chemical Society*, 2015. doi: 10.1021/cr500279h
- [105] G. Bagni, M. Ravera, D. Osella, and M. Mascini, "Electrochemical Biosensors as a Screening Tool of In Vitro DNA-Drug Interaction," *Current Pharmaceutical Analysis*, vol. 1, no. 3, pp. 217–224, Oct. 2005, doi: 10.2174/157341205774597904.
- [106] A. H. Wang, G. Ughetto, G. J. Quigley, and A. Rich, "Interactions between an Anthracycline Antibiotic and DNA: Molecular Structure of Daunomycin Complexed to d(CpGpTpApCpG) at 1.2-Å Resolution," *Biochemistry*, vol. 26, no. 4, pp. 1152–1163, 1987, doi: 10.1021/BI00378A025.
- [107] A. M. O. Brett, T. R. A. MacEdo, D. Raimundo, M. H. Marques, and S. H. P. Serrano, "Voltammetric behaviour of mitoxantrone at a DNA-biosensor," *Biosensors and Bioelectronics*, vol. 13, no. 7–8, pp. 861–867, Oct. 1998, doi: 10.1016/S0956-5663(98)00053-0.
- [108] U. Eskiocak, D. Ozkan-Ariksoysal, M. Ozsoz, and H. A. Öktem, "Label-Free Detection of Telomerase Activity Using Guanine Electrochemical Oxidation Signal," *Analytical Chemistry*, vol. 79, no. 22, pp. 8807–8811, Nov. 2007, doi: 10.1021/AC071014R.
- [109] M. Ozsoz, A. Erdem, P. Kara, K. Kerman, and D. Ozkan, "Electrochemical Biosensor for the Detection of Interaction Between Arsenic Trioxide and

- DNA Based on Guanine Signal,” *Electroanalysis*, vol. 15, no. 7, pp. 613–619, May 2003, doi: 10.1002/ELAN.200390077.
- [110] Y. Yardım, M. Vandeput, M. Çelebi, Z. Şentürk, and J. M. Kauffmann, “A Reduced Graphene Oxide-based Electrochemical DNA Biosensor for the Detection of Interaction between Cisplatin and DNA based on Guanine and Adenine Oxidation Signals,” *Electroanalysis*, vol. 29, no. 5, pp. 1451–1458, May 2017, doi: 10.1002/ELAN.201600804.
- [111] P. Du, H. Li, Z. Mei, and S. Liu, “Electrochemical DNA biosensor for the detection of DNA hybridization with the amplification of Au nanoparticles and CdS nanoparticles,” *Bioelectrochemistry*, vol. 75, no. 1, pp. 37–43, Apr. 2009, doi: 10.1016/J.BIOELECTCHEM.2009.01.003.
- [112] Y. Qian, C. Wang, F. G. Talanta,, “Enzyme-free amplification for sensitive electrochemical detection of DNA via target-catalyzed hairpin assembly assisted current change,” *Elsevier*, 2014.
- [113] C. Witte, F. L.- Electroanalysis, and undefined 2011, “Direct Detection of DNA and DNA- ligand interaction by impedance spectroscopy,” *Wiley Online Library*, vol. 23, no. 2, pp. 339–346, Feb. 2011, doi: 10.1002/elan.201000410.
- [114] M. Khater, A. de la Escosura-Muñiz, D. Quesada-González, and A. Merkoçi, “Electrochemical detection of plant virus using gold nanoparticle-modified electrodes,” *Analytica Chimica Acta*, vol. 1046, pp. 123–131, Jan. 2019, doi: 10.1016/J.ACA.2018.09.031.
- [115] T. Liu, J. Tang, and L. Jiang, “The enhancement effect of gold nanoparticles as a surface modifier on DNA sensor sensitivity,” *Biochemical and Biophysical Research Communications*, vol. 313, no. 1, pp. 3–7, Jan. 2004, doi: 10.1016/J.BBRC.2003.11.098.

- [116] Q. Zhang, P. Dai, and Z. Yang, "Sensitive DNA-hybridization biosensors based on gold nanoparticles for testing DNA damage by Cd(II) ions," *Microchimica Acta*, vol. 173, no. 3–4, pp. 347–352, Jun. 2011.
- [117] S. Fathi *et al.*, "Novel Competitive Voltammetric Aptasensor Based on Electrospun Carbon Nanofibers-Gold Nanoparticles Modified Graphite Electrode for Salmonella enterica serovar Detection," vol. 11, no. 1, pp. 8702–8715, 2021, doi: 10.33263/BRIAC112.87028715.
- [118] C. Liu, D. Jiang, G. Xiang, L. Liu, F. Liu, and X. Pu, "An electrochemical DNA biosensor for the detection of Mycobacterium tuberculosis, based on signal amplification of graphene and a gold nanoparticle–polyaniline nanocomposite," *Analyst*, vol. 139, no. 21, pp. 5460–5465, Sep. 2014, doi: 10.1039/C4AN00976B.
- [119] T. Jantararat *et al.*, "A Label-free DNA-based Fluorescent Sensor for Cisplatin Detection," *Sensors and Actuators B: Chemical*, vol. 326, p. 128764, Jan. 2021, doi: 10.1016/J.SNB.2020.128764.
- [120] S. K. K. Galagedera and G. U. Flechsig, "Detection of the level of DNA cross-linking with cisplatin by electrochemical quartz crystal microbalance," *Journal of Electroanalytical Chemistry*, vol. 862, p. 113992, Apr. 2020, doi: 10.1016/J.JELECHEM.2020.113992.
- [121] D. Zhao, J. Li, T. Yang, and Z. He, "'Turn off–on' fluorescent sensor for platinum drugs-DNA interactions based on quantum dots," *Biosensors and Bioelectronics*, vol. 52, pp. 29–35, Feb. 2014, doi: 10.1016/J.BIOS.2013.08.031.
- [122] H. Kostrhunova, O. Vrana, T. Suchankova, D. Gibson, J. Kasparkova, and V. Brabec, "Different features of the DNA binding mode of antitumor cis - amminedichlorido(cyclohexylamine)platinum(II) (JM118) and cisplatin in vitro," *Chemical Research in Toxicology*, vol. 23, no. 11, pp. 1833–1842, Nov. 2010.

- [123] M. M. El-Wakil, M. Darweesh, M. S. A. Shaykoon, and R. Ali, “Enzyme-free and label-free strategy for electrochemical oxaliplatin aptasensing by using rGO/MWCNTs loaded with AuPd nanoparticles as signal probes and electro-catalytic enhancers,” *Talanta*, vol. 217, p. 121084, Sep. 2020, doi: 10.1016/J.TALANTA.2020.121084.
- [124] M. Abdul Aziz and A. N. Kawde, “Gold nanoparticle-modified graphite pencil electrode for the high-sensitivity detection of hydrazine,” *Talanta*, vol. 115, pp. 214–221, Oct. 2013, doi: 10.1016/J.TALANTA.2013.04.038.
- [125] J. Mohanty, N. Barooah, V. Dhamodharan, S. Harikrishna, P. I. Pradeepkumar, and A. C. Bhasikuttan, “Thioflavin T as an efficient inducer and selective fluorescent sensor for the human telomeric G-quadruplex DNA,” *J Am Chem Soc*, vol. 135, no. 1, pp. 367–376, Jan. 2013, doi: 10.1021/JA309588H.
- [126] X. F. Zhang, H. M. Xu, L. Han, N. B. Li, and H. Q. Luo, “A Thioflavin T-induced G-Quadruplex Fluorescent Biosensor for Target DNA Detection,” *Anal Sci*, vol. 34, no. 2, pp. 149–153, 2018, doi: 10.2116/ANALSCI.34.149.
- [127] A. R. de La Faverie, A. Guédin, A. Bedrat, L. A. Yatsunyk, and J. L. Mergny, “Thioflavin T as a fluorescence light-up probe for G4 formation,” *Nucleic Acids Research*, vol. 42, no. 8, 2014, doi: 10.1093/NAR/GKU111.
- [128] P. Yaşar *et al.*, “A CpG island promoter drives the CXXC5 gene expression,” *Scientific Reports* /, vol. 11, p. 15655, 123AD, doi: 10.1038/s41598-021-95165-6.
- [129] A. Marchand, F. Rosu, R. Zenobi, and V. Gabelica, “Thermal Denaturation of DNA G-Quadruplexes and Their Complexes with Ligands: Thermodynamic Analysis of the Multiple States Revealed by Mass Spectrometry,” *J Am Chem Soc*, vol. 140, no. 39, pp. 12553–12565, Oct. 2018.

- [130] S. Paramasivan, I. Rujan, and P. H. Bolton, “Circular dichroism of quadruplex DNAs: Applications to structure, cation effects and ligand binding,” *Methods*, vol. 43, no. 4, pp. 324–331, Dec. 2007, doi: 10.1016/J.YMETH.2007.02.009.
- [131] P. Agrawal, E. Hatzakis, K. Guo, M. Carver, and D. Yang, “Solution structure of the major G-quadruplex formed in the human VEGF promoter in K⁺: insights into loop interactions of the parallel G-quadruplexes,” *Nucleic Acids Research*, vol. 41, no. 22, p. 10584, Dec. 2013, doi: 10.1093/NAR/GKT784.
- [132] J. Chaires and D. Graves, “Quadruplex nucleic acids,” *Springer-Verlag*, 2013.
- [133] R. del Villar-Guerra, J. O. Trent, and J. B. Chaires, “G-Quadruplex Secondary Structure Obtained from Circular Dichroism Spectroscopy,” *Angewandte Chemie International Edition*, vol. 57, no. 24, pp. 7171–7175, Jun. 2018, doi: 10.1002/ANIE.201709184.